NEW PARTICLE SEARCHES AT PEP

D. Berley, F. Bulos, D. Cheng, B. Cork, P. Limon,

A. Litke, U. Nauenberg, J. Rosen, B. Shen,

L. Sulak, J. Trefil, F. Winkelmann

ABSTRACT

The new particles that could be produced at PEP are dis-
cussed in terms of their specific signatures and production
rates. We find that a small number of general signatures
characterize these particles. Backgrounds associated with
the general signatures are considered and necessary rejection
rates are calculated. We describe several typical detectors
and tabulate the requirements they place on the PEP machine and the
experimental areas.

CONTENTS

I   <u>INTRODUCTION</u>

We identify general signatures for new particles by first investigating the specific signatures of the conventionally sought particles. We then investigate the backgrounds which would mimic the lepton-lepton and lepton-hadron signatures. Lastly, we design several typical detectors that are sensitive to the general signatures. These apparatus illustrate the requirements placed on the PEP machine and experimental areas by the detectors.

II SPECIFIC SIGNATURES OF NEW PARTICLES

We have investigated the conventional new particles and summarize their properties in this section and in Tables 1-11. The particles considered are the following:

(1) Heavy leptons - excited, sequential, gauge theory, and quasi-stable heavy leptons

(2) Charged Intermediate Vector Bosons

(3) Charmed Hadrons

(4) Resonances

(5) Quarks

(6) Gluons

(7) Monopoles

(8) Higgs Scalars

(9) Neutral Intermediate Bosons

(10) Lee-Wick Particles

(11) Tachyons

The numbering of the tables and the subsections of this section are the same. The references in this section and in the tables appear at the bottom of each appropriate table.

In estimating particle production rates, we have quantized the duration of an experiment in terms of the yield of $e^+e^- \to \mu^+\mu^-$ events. We chose 10^4 events ($\approx$ an integrated luminosity of 10^{38} cm^2) as a typical exposure. For the design luminosity expected at PEP, and an appropriate factor for machine down time, etc, this number of $\mu^+\mu^-$ pairs is accumulated in 40-300 days.

We summarize the impact on PEP of the data presented in the next eleven subsections:

1) Significant new lower limits (an order of magnitude better than presently available) can be set on excited heavy leptons, sequential heavy leptons, the E^0 gauge-theory heavy lepton, quasi-stable heavy leptons, charmed hadrons, high mass resonances, and Higg's scalars. The possible new PEP limits on the other particles considered are not significant. In particular, the mass of the directly produced W boson, whether electromagnetically or weakly produced at PEP, is not superior to the present lower limits set by the FNAL neutrino experiments.

2) The salient signatures are <u>acoplanar</u> lepton pairs (radiative corrections produce <u>coplanar</u> ee and $\mu\mu$ pairs), single leptons, missing transverse momentum $(P_\perp)$, and anomalous strange particle production.

3) Events rates per typical experiment are high: 100 lepton-lepton pairs and/or 1000 lepton-hadron events.

(1) HEAVY LEPTONS

The heavy leptons can be classified into three groups according to their leptonic number properties: (i) excited leptons, (ii) sequential leptons, and (iii) guage theory leptons. At PEP new charged leptons are produced electromagnetically just as muon pairs are produced. Hence, the cross section for charged heavy lepton pair production is identical to that for muon pair production, except for a kinematic threshold factor ($\frac{3\beta-\beta^3}{2}$, where β = velocity of the lepton in CMS) and possibly a form factor. Since the threshold factor is already 0.7 at $\beta = 0.5$, the production rates are quite high and are comparable to the $\mu^+\mu^-$ rate. At PEP energies new neutral heavy leptons, including heavy neutrinos, can be produced via weak interactions with cross sections about one to two orders of magnitude lower than that of muon pair production. All the heavy leptons are expected to decay with a short lifetime. However, the possibility that any of the above leptons are quasi-stable cannot be ruled out.

(i) Excited Leptons

Excited leptons $(\ell,\ell^*,\ldots;\nu_\ell,\nu_\ell^*,\ldots)$ have the same set of leptonic numbers as the lepton ℓ (electron or muon). Hence, these leptons decay almost 100% of the time electromagnetically into their lower mass states:

$$\ell^* \rightarrow \ell + \gamma .$$

Heavy excited neutrinos would be produced by weak interactions $e^+e^- \rightarrow \nu_\ell^* \overline{\nu_\ell^*}$, and decay weakly:

$$\nu_\ell^* \rightarrow \ell^-(\ell^+\nu_\ell)$$
$$\rightarrow \ell^- + hadrons$$

(ii) Sequential Leptons

Sequential leptons are similar to excited leptons except that their leptonic numbers are different fromthose of the electron and muon, and they possess their own associated neutrinos. They can decay in pure leptonic modes as well as in semi-leptonic modes:
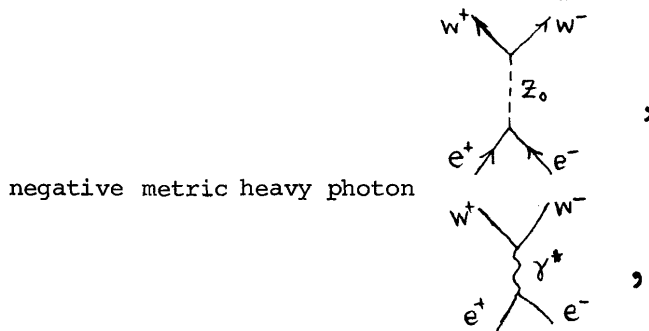
$$\ell'^{-} \rightarrow \nu'_{\ell}(\ell^{-}\overline{\nu_{\ell}})$$

$$\rightarrow \nu'_{\ell} + hadrons$$

(iii) <u>Gauge Theory Leptons</u>

The non-gauge theories of the weak interaction suffer from divergence

difficulties in reactions such as $e^{+}e^{-} \rightarrow W^{+}W^{-}$:
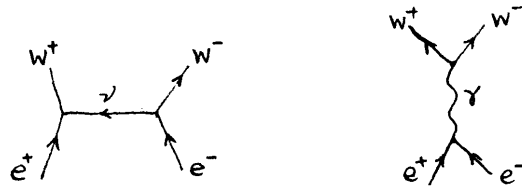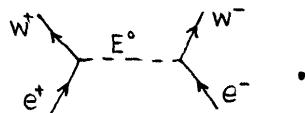

These difficulties can be cured by the introduction of neutral current

negative metric heavy photon

or heavy lepton

In particular, both the Georgi-Glashow and Lee-Prentki-Zumino models require

the existence of heavy leptons. The gauge heavy lepton with positive charge L+

(M^{+}) has the same leptonic number as that of the electron(or muon) . The

decay modes of these leptons are very similar to those of the sequential

leptons.

For certain gauge models the existence of neutral heavy leptons (L^{o})

is also required. It is likely that the mass of the L^{o} is much lighter than

that of the L^{+} (e.g., Georgi-Glashow model, $m_{L^{o}} \sim 0.5\ m_{L^{+}}$). Hence, the L^{o}

might be directly produced at PEP, even though $L^{\pm}$ might be too massive.

Neutral gauge leptons are weakly produced as pairs $(e^{+}e^{-} \rightarrow L^{o}\overline{L^{o}})$, or singly

456

$(e^+e^- \to L^0\bar{\nu}_\ell)$. In the second mode, much more massive L^0's can be produced

than in the first. Production cross sections for these processes are model

dependent. For the Georgi-Glashow model,

$$\sigma(L^0\overline{L^0}) \cong \frac{G_F^2 S(1-4\ M_{E^0}^2/S)^{1/2}}{2\pi \sin^2 \theta_G} \ [\frac{1}{3}(1 - \frac{M_{E^0}^2}{S})(1 + \cos^4 \theta_G) + 2 \cos^2 \theta_G(1 - \frac{2M_{E^0}^2}{S}] \ ,$$

and

$$\sigma(L^0\bar{\nu}_\ell) \cong \frac{G_F^2 S(1 - \frac{M_{E^0}^2}{S})^2}{2\pi \sin^2 \theta_G} \cdot [1 + \frac{1}{3} \cos^2 \theta_G(1 + \frac{M_{E^0}^2}{2S})] \ ,$$

where $\sin \theta_G = M_W/53$ GeV, and $M_{E^0} \ll M_W$. Compared with the muon-pair produc-

tion cross section at $\sqrt{S} = 30$ GeV we have

$$\sigma(L^0\overline{L^0})/\sigma(\mu^+\mu^-) \gtrsim 0.043 \qquad \text{for} \qquad M_{L^0} = 14 \text{ GeV}/c^2$$

and

$$\sigma(L^0\bar{\nu}_\ell)/\sigma(\mu^+\mu^-) \gtrsim 0.023 \qquad \text{for} \qquad M_{L^0} = 20 \text{ GeV}/c^2$$

Summary

All the charged heavy leptons discussed above have a common leptonic decay

signature: acolinear and acoplanar lepton pairs. In addition, neutral heavy

leptons have the same signature, and could have four charged leptons in the

final state. Since radiative corrections can introduce a substantial amount

of acolinearity, the search for acoplanar lepton pairs would be the best way

to look for these particles. If the axial vector current is not too different

from the weak vector current, the branching ratio can be estimated using SPEAR II

results for the electromagnetic vector current:[†]

[†]We thank Prof. S. Treiman for calling our attention to this argument

457

$$\frac{\Gamma(L \rightarrow \text{ only leptons})}{\Gamma(L \rightarrow \nu + \text{hadrons})} \sim \frac{\sigma(W \rightarrow \ell \nu)}{\sigma(W \rightarrow \text{hadrons})} \sim \left.\frac{\sigma(\gamma \rightarrow \mu^+\mu^-)}{\sigma(\gamma \rightarrow \text{hadrons})}\right|_{M_\gamma \approx \frac{M_L}{2}} \equiv \left.\frac{1}{R(s)}\right|_{\sqrt{s} \approx \frac{M_L}{2}}$$

where $R(S) \equiv \dfrac{\sigma(e^+e^- \rightarrow \text{hadrons})}{\sigma(e^+e^- \rightarrow \mu^+\mu^-)}$ $\quad (\approx 5 \quad \text{at} \quad \sqrt{s} = 5 \text{ GeV})$

If, for some unforeseen reason, the purely leptonic decay mode is suppressed, one can search for the more difficult signature of a single charged lepton among the hadrons (one heavy lepton decays leptonically while the other decays hadronically). When both heavy leptons decay hadronically, one can search for the missing energy and momentum carried off by the two undetected neutrinos. Since much of the momentum of the hadrons in the conventional $e^+e^- \rightarrow$ h's can disappear into the beam pipe (particularly from 2-photon processes), the background from these processes would be lower in a search for missing momentum perpendicular to the beam pipe.

Any of the leptons listed above could be quasistable and not decay in a typical detector. The signature for such leptons when produced in pairs is a massive, penetrating collinear pair of particles.

(2) CHARGED INTERMEDIATE VECTOR BOSONS

The signature for many processes proceeding via the weak interaction is a muon and an electron in the final state. This signature is a powerful filter against purely hadronic processes and, in the absence of heavy leptons, could be exploited to study the weak interactions to a level of $^{\sim}10^{-4}$ of the quasi-elastic $\mu\mu$ process. Weak interaction experiments are limited by the projected PEP luminosity of $L = 10^{32} \sec^{-1} cm^{-2}$, which corresponds to an effective average annual luminosity of 10^{38} year^{-1} cm^{-2}. We will show that the rate for weak interaction events is no more than a few per year.

The Production of W's via Electromagnetism

One possibility to study the weak interactions is by the direct production of W^+W^- pairs via photon exchange:

The cross section for the this process is

$$\sigma_{W^+W^-} = \left(\frac{1}{M_W}\right)^2 (2.1 \times 10^{-32}) \frac{3}{4}\left(1 - \frac{4M_W^2}{E^2}\right)^{3/2}\left(\frac{4}{3} + \frac{4M_W^2}{E^2}\right), \quad (1)$$

where $M_W=$ the boson mass and

2E= the total energy in C.M. (5<E<15 GeV for PEP).

It is assumed that the anomolus magnetic dipole and electric quadrupole moments are both zero, and that the form factors have their static values. If form factor variations are neglected there are no combinations of the anomolous moments which substantially reduce $\sigma_{W^+W^-}$ below that given by equation (1).

By comparison, the annihilation cross section into charged fermion pairs is[1]

$$\sigma_{f^+f^-} = \left(\frac{1}{E}\right)^2 \left(2.1 \times 10^{-32}\right)\left[1 - \left(\frac{m_f}{E}\right)^2\right]^{1/2}\left[1 + \frac{1}{2}\left(\frac{m_f}{E}\right)^2\right],$$

where M_f = the fermion mass.

For muon pairs

$$\sigma_{\mu\mu} = \frac{2.1 \times 10^{-32}}{E^2}$$

for $E \gg m_\mu$, and the ratio

$$\frac{\sigma_{W^+W^-}}{\sigma_{\mu\mu}} = \left(\frac{E}{4M_W}\right)^2 \frac{3}{4}\left(1 - \frac{4M_W^2}{E^2}\right)^{3/2}\left(\frac{4}{3} + \frac{4M_W^2}{E^2}\right)$$

is plotted in Figure 1. Also shown is the expected number of events per year. More than 1000 events/year are produced if the boson mass is less than 13.2 GeV. The rates for W pair production are enormous for $M_W \lesssim 14$ GeV!

Present Limits on the W Mass

The best limits on the mass of the W come from two experiments:

1. The linearity of the total νN cross section measured with neutrino energies up to 200 GeV gives[2] $M_W \gtrsim 13$ GeV.

2. A search for the production of high transverse momentum muons in pp collisions at the ISR[3] (pp→μ+X) gives $M_W \gtrsim 18$-24 GeV. Both of these depend on models for their interpretation and a search for W production via a more certain production mechanism would be worthwhile.

W Production Through The Weak Interaction.

$W^\pm$ production up to $M_W \approx 2E_0 = 30$ GeV is possible in the reaction

$$e^+e^- \to e^\pm\nu\, W^\mp \quad.$$

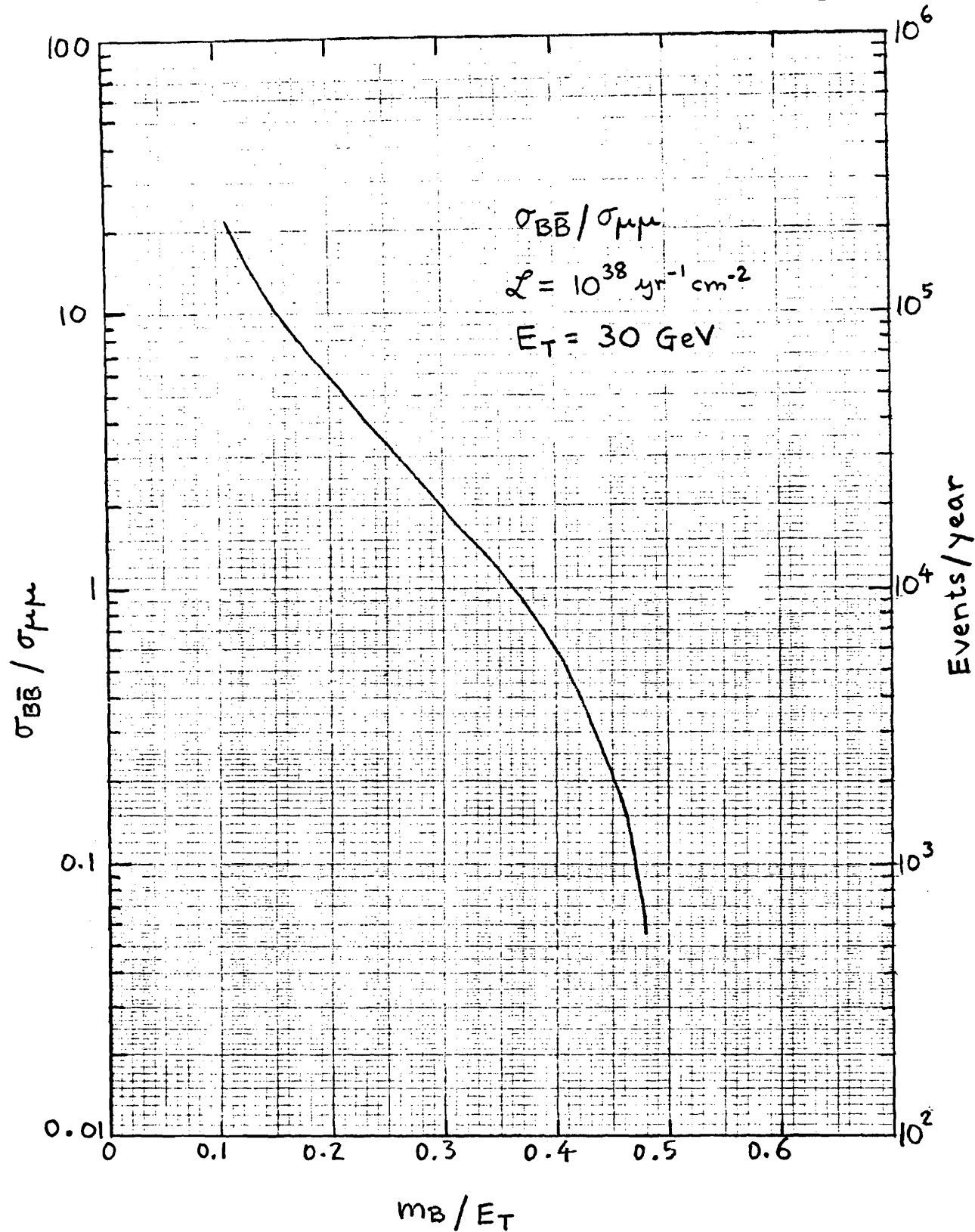The dominant Feynman diagrams for this process are [4,5]

460
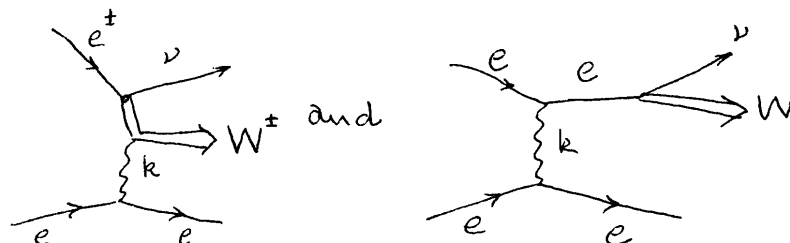
FIGURE 1

461

and the cross section is[6]

$$\frac{d^2\sigma}{dM_{W\nu}^2 dk^2} = \frac{1}{32\pi} \left[\frac{G M_W^2 \alpha^2}{\sqrt{2}\, E^2} \right]^2 \frac{M_{W\nu}^2 - M_W^2}{M_{W\nu}^2} \frac{M_W^2}{k^4} \times$$

$$\times U\left(\frac{M_W^2}{M_{W\nu}^2}, \frac{M_W^2}{k^2} \right) + O\left(\frac{m_e}{k}, \frac{m_e}{m_W}, \frac{m_e}{E} \right).$$

Here

G = Fermi weak coupling constant $\cong 10^{-5}\, m_p^{-2}$,

$M_{W\nu}$ = invariant mass of $W\nu$ system,

k = momentum transferred to the final state electron or positron,

$$U\left(\frac{M_W^2}{M_{W\nu}^2}, \frac{M_W^2}{k^2} \right) = \text{a function of } \frac{M_W^2}{M_{W\nu}^2} \text{ and } \frac{M_W^2}{k^2},$$

$$O\left(\frac{m_e}{k}, \frac{m_e}{M_W}, \frac{m_e}{E} \right) = \text{terms of the order } M_e/M_W, \text{ etc., and neglected.}$$

The total cross section,

$$\sigma_{e^\pm \nu\, W^\mp} = \int \frac{d^2\sigma}{dM_{W\nu}^2 dk^2}\, dM_{W\nu}^2\, dk^2,$$

is a function of M_W/E only! We therefore use the single W cross sections

calculated by Berends and West[4] for energies 3<E<7 GeV. These are plotted

in Figure 2.

For 12<M_W<18 GeV we expect between 1 and 10 events/year, which is too

low to be practical. Therefore the expected PEP luminosity is too low to study

W production   processes with a weak interaction vertex.
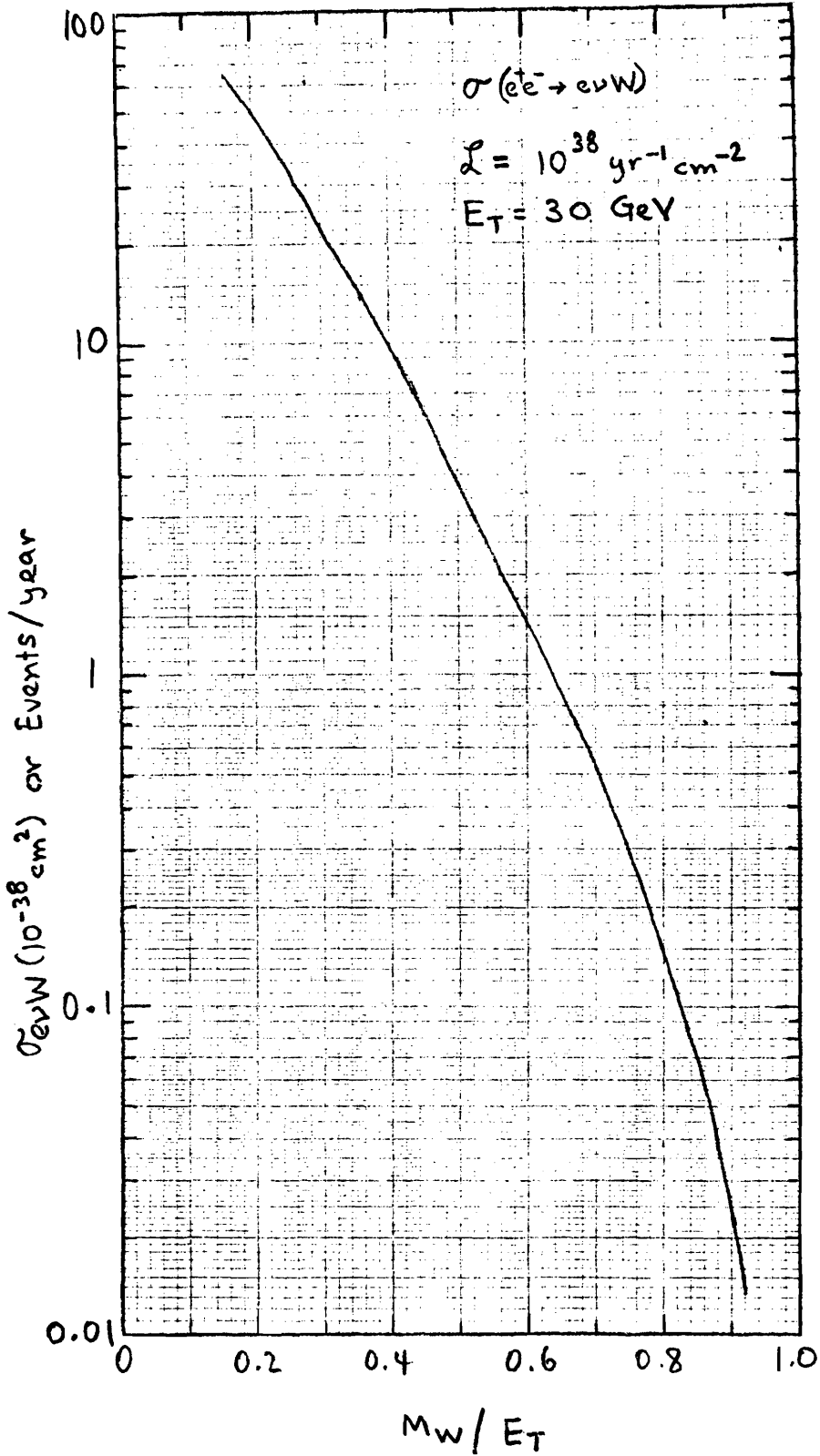
FIGURE 2

(3) CHARMED PARTICLES

Charm is a new quantum number, characteristic of a fourth quark (p') in the standard Gell-Mann picture. It was invented to suppress $\Delta S \neq 0$ neutral currents such as $K_L^o \rightarrow \mu\mu$. In order to cancel the standard charged current

$$J^+ = \bar{p}(n\cos\theta_c + \lambda\sin\theta_c) + \bar{\nu}_\mu\mu + \bar{\nu}_e e, \quad (1)$$

another term must be added

$$J_c = \bar{p}'(\lambda\cos\theta_c - n\sin\theta_c). \quad (2)$$

For (1) alone a neutral current would induce a term in $K_L^o \rightarrow \mu\mu$ which would make its rate comparable to $K^+ \rightarrow \mu^+\nu_\mu$.

The p' has the charge of the p quark, $I = 0$, $S = 0$, and a new quantum number, charm $C = 1$. Equation (2) implies that the p' couples as $\cos\theta_c$ to λ, so its weak decay into strong particles is not suppressed, in contrast to normal baryons which are coupled as $\sin\theta_c$ to strange quarks.

The second order amplitudes for the weak decay of K mesons into neutral lepton pairs ($K_L^o \rightarrow \pi^o\nu\bar{\nu}$, $\mu\mu$, etc.), for the $K_L - K_S$ mass difference, and for $K_L^o \rightarrow \gamma\gamma$ decay yield a limit on the mass of the p' quark:

$$M_{p'}^2 \approx M_{p'}^2 - M_p^2 \ll M_W \sin^2\theta_W \approx (38 \text{ GeV})^2,$$

Evaluating these amplitudes using _free_ quark diagrams gives

$$M_p \lesssim M_k \ll M_{p'} \lesssim 2 \text{ GeV}$$

The charmed particle mass is limited from above by requiring that it produce cancellations appropriate to the low

$K_L \rightarrow \mu^+\mu^-$ rates. Estimates of charmed particle masses thus re-
strain M_c :

$$2 \text{ GeV} \lesssim M_c \lesssim 10 \text{ GeV}.$$

Since the p' couples as $\cos \theta_c$ to λ, one expects copious
production of strong particles from their weak decay.

The lifetimes are expected to be short, $\approx 10^{-12}$ or 10^{-13} sec
due to this large decay amplitude, and the high mass of the par-
ticles.

No suppression of the leptonic decay modes relative to the
non-leptonic, as in the case for strange particles, is expected.
Therefore, we expect (1) a large branching ratio into strange par-
ticles associated either with another hadron or a lepton neu-
trino pair or (2) two lepton neutrino pairs and hadrons.

PEP enjoys an advantage of FNAL and the ISR in charm parti-
cle searches. Since no charmed valence quarks or strange valence
quarks exist in ordinary targets, neutrino or lepton production
of charmed particles is suppressed by $\sin \theta_c$. In e^+e^- collisions,
if we ignore phase space factors (i.e. are well above threshold),
we expect charmed particles to be produced at the same rate, or
higher, than strange particles. From simple quark counting, we
expect, below the charmed particle threshold, that 10% of the
hadrons produced would be strange particles. Above the charmed
threshold, 40% of the hadrons would have charm (since $Q_{p'}^2 = (2/3)^2$
and $Q_\lambda^2 = (1/3)^2$). Since all of the charmed particles decay into
strange particles, perhaps 50% of the visible hadrons would have
characteristic strange particle decays. The production rates at
PEP energies are unknown and uncalculable except for free quark
models with no form factors.

(4) RESONANCES

Resonant states can be produced in e^+e^- collisions via three distinct processes: (a) s-channel formation, (b) two photon exchange, and (c) production in multiparticle final states. We discuss these in turn.

(a) s-channel formation

The relevent diagram is
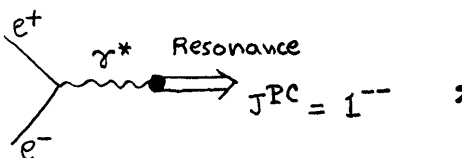
where the resonance couples directly to the virtual photon and therefore has $J^{PC} = 1^{--}$. Resonance formation would appear as a bump (at $2E_0$ = resonance mass) in the cross section vs. beam energy, E_0, for $e^+e^- \to$ specific final state. To search for charmed resonances, for example, one might inspect σ vs. E_0 for final states with several strange particles. The higher vector mesons (ρ', ω', and ϕ') [1] are likely to be too closely spaced ($\Delta E_0 \sim 15$ MeV) and too broad ($\Gamma \gtrsim 400$ MeV) to be easily detectable at PEP.
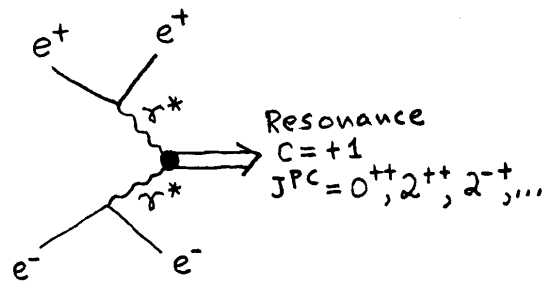
Resonances which couple to the photon can be investigated <u>at a single beam energy</u> using the process
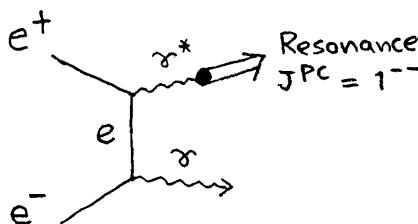
However, the cross section here is down by α^2 relative to the single photon channel and good γ detection and measurement is required.

(b) <u>Two-photon exchange</u>

In the two-photon exchange process

resonances can be formed which couple to the $\gamma\gamma$ system and therefore have

$C = +1$. The allowed J^{PC} states are 0^{++}, 2^{++}, 2^{-+}, etc. (Since the two

photons are almost real, $J = 1$ states are suppressed.) Relative to the single

photon channel, rates for the two-photon process are down by α^2 but are

enhanced by a $[\ln(E_0/M_e)]^2$ factor.

Precise measurement of the outgoing $e^{\pm}$ is clearly required to determine

the invariant mass M of the produced particles. However, a broad range of M

is, in principle, available for fixed E_0, so that a beam energy sweep is not

required to search for resonance bumps.

(c) <u>Production in multiparticle final states</u>

Both the one- and two-photon channels can contribute to final

states containing resonances plus other produced particles:
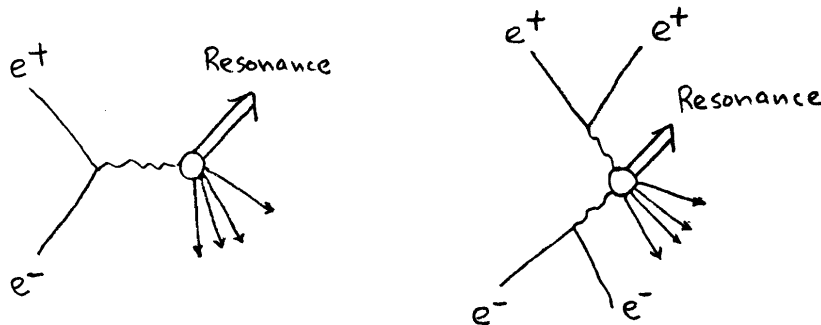
In this case, resonances would be revealed as structure in invariant mass or missing mass distributions for specific final states or for inclusive processes. As an illustration, consider the production of an excited electron, e^*, in the reaction

$$e^+ e^- \rightarrow e^{*-} e^+$$
$$\quad \rightarrow e^- \gamma \quad .$$
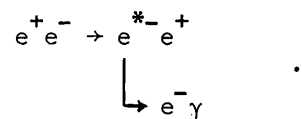
If the outgoing e^- and γ are measured, the e^{*-} would appear as a peak in the $e^- \gamma$ invariant mass distribution. If, on the other hand, the γ is undetected, one could choose events with an acoplanar $e^+ e^-$ pair and search for a peak in the distribution of missing mass against the outgoing e^+.

(5) QUARKS

Cross Section

Quark pair production via
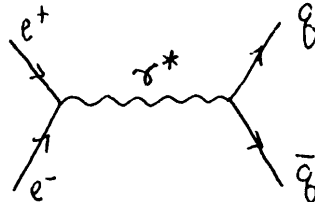
allows quarks of mass up to ~ 15 GeV to be produced at PEP. For spin-1/2, pointlike quarks,

$$\sigma(e^+e^- \rightarrow q\bar{q}) \approx Z^2(\frac{3\beta-\beta^3}{2})\sigma(e^+e^- \rightarrow \mu^+\mu^-) \ ,$$

where Z is the quark charge and $\beta = v/c = [1 - (M_q/E_o)^2]^{1/2}$. Choosing $Z = 2/3$ and requiring $M_q > 4.3$ GeV (as suggested by the observed cross sections of $\lesssim 10^{-37}$ cm^2 for $pp \rightarrow q\bar{q}X$ [1]), we find

$$\sigma_{q\bar{q}} \lesssim 0.64 \ \sigma_{\mu\mu}$$

for $E_o = 10$ GeV. Thus quark-pair and μ-pair production at PEP could be comparable.

Signatures

Free quarks, if quasi-stable, could be detected as a colinear particle pair. Fractionally charged quasi-stable quarks would, in addition, have anomalous dE/dx since energy loss by electromagnetic processes is proportional to Z^2. For sufficiently massive quarks a time-of-flight measurement would give β and thus the quark mass, using $M_q = E_o\sqrt{1-\beta^2}$. If β is not measured directly, then both the quark charge (from dE/dx) and momentum (from charge plus curvature in a magnetic field) have to be measured to obtain M_q.

For unstable quarks, a colinear pair of hadron jets would be the signature for $q\bar{q}$ production.

---

[1] J. S. Trefil, Appendix A

(6)   THE GLUON

Although the existence of a neutral vector field for renormalizable strong interactions has been discussed[1-3], the existence and hence properties of a particle (the gluon) corresponding to this neutral vector field have only been speculated. In the simplest case, the gluon is an SU_3 singlet,[4] massive, vector boson.

Since the gluon is an SU_3 singlet, it does not couple directly to the electromagnetic current and thus the rate of formation in e^+e^- collisions is expected to be small.

Furthermore, the gluon cannot be formed via two-photon annihilation processes since it is expected to have an odd charge conjugation quantum number. However, if it is formed, the mass limit at PEP is about 28 GeV/c^2.

There is no clear signature for the observation of a gluon. It may show up as a bump in the total hadronic cross section as a function of cm energy of the e^+e^-. Since it couples strongly to hadrons it may have a large width. One may also measure specific final state cross sections as a function of energy. There is no experimental mass limit at present.
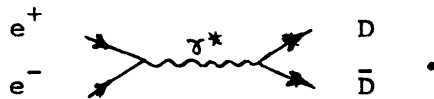
(7) MONOPOLES

Magnetic monopoles were first suggested [1] in an attempt to explain the quantization of the electric charge through the relationship

$$\frac{ge}{\hbar c} = \frac{n}{2},$$

where g is the strength of the magnetic monopole, e is the electric charge and n is an integer. The coupling of the magnetic monopole to the electromagnetic field is very strong, typically of the order of α^{-1}. Schwinger proposed that the basic constituents of matter, such as quarks, can also carry magnetic charge in fractional units of g. These were referred to as 'dyons' [2], and designated by the symbol $^{2/3}D^{-1/3}$, for example, for a dyon of 2/3 magnetic charge and -1/3 e electric charge. For simplicity in notation, a magnetic pole will be designated by D hereafter.

To conserve magnetic charge, monopoles are most likely produced electromagnetically in pairs, namely,

Since the coupling strength is super-strong, there is no reliable way to estimate the production cross section. Nothing has been predicted about the spin and other intrinsic quantum numbers of the magnetic monopoles. The mass of the monopole has been estimated to be from a few GeV [2] to 137 x M_W.

Although it is possible that magnetic monopoles may be detected as free particles, it is more likely [4] that the oppositely charged $D\bar{D}$ pair will have a strong mutual attraction and tend to recombine, annihilating into γ's or even into hadrons in the case of dyon pair production:

471

$e^+ e^- \to D\bar{D} \to \gamma\text{'s}$ or $e^+ e^- \to D\bar{D} \to \text{hadrons}$.
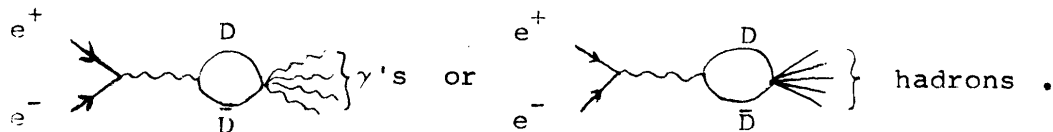
This may explain why monopoles have not been observed direct-ly.

Experimental signatures for free monopoles are: (i) its magnetic charge (thus it is accelerated in a magnetic field and induces electromotive force when passing through a supercon-ducting coil; (ii) its heavy ionization in matter and Cerenkov ra-diation (with an electric vector field rotated by 90 degrees). If $D\bar{D}$ pairs annihilate into γ's, the signature would then be a large number of γ's carrying the entire cm energy.

Present experimental limits come from a number of vastly dif-ferent experiments: searching moon rock [5], ocean bottom [6], and nucleon-nucleon collisons at high energy accel rators [7]. The production cross section for free monopoles of $M_D \leq 5$ GeV is less than 1.4×10^{-43} cm^2 in pN $\to$ pN $D\bar{D}$ [7].

(8)(9) **HIGGS SCALAR AND NEUTRAL INTERMEDIATE BOSON**

The massive neutral intermediate vector boson[1] and the Higgs scalar meson[2] are suggested in gauge theories. They may be formed electromagnetically in pairs in e^+e^- collisions. The production rates of Z^0 and $\bar{\phi}$ are model dependent and ex-pected to be quite small (~1 percent of $e^+e^- \to \mu^+\mu^-$). The mass limit at PEP is approximately 30 GeV. However, since the decay is electromagnetic, the width would be small. The experimental signature would be a sharp peak in the $\mu\mu^-$ or ee^- cross sections

as a function of cm energy.[3] The present limit on $\hat{\Phi}$ is
$M_{\hat{\Phi}} > 0.5$ GeV[4]. There is no experimental limit on the mass of
Z^0 but it is expected that $M_{Z^0} \approx 80$ GeV in some models.[1] Per-
haps the best place to search for the Z^0 is in the interference
between it and the photon in $\mu\mu$ production.

(10) HEAVY PHOTONS AND LEE-WICK PARTICLES

Coulomb's Law, as is well known, is intimately related to the fact
that the photon has zero mass. The existence of a massive photon which
couples to the electromagnetic current would cause deviations from
Coulomb's Law at short distances. If a heavy photon of mass Λ_+ exists
then the usual photon propagator $1/q^2$ must be replaced by $1/q^2 + 1/(q^2-\Lambda_+^2)$.
This modified propagator would lead to a breakdown of QED at large
momentum transfers.

In order to clear up divergence problems in the calculation of
radiative corrections to weak interactions and in the calculation of
electromagnetic mass splittings, Lee and Wick[5] introduced a negative
metric vector boson. The coupling of this particle to the electromagnetic
current modifies the photon propagator to $1/q^2-1/(q^2-\Lambda_-^2)$, where Λ_- is the
mass of the Lee-Wick particle. At high q^2 this modified propagator falls
off as q^{-4}; this is useful for damping the divergences mentioned above.

Heavy photons and Lee-Wick particles, if they exist, can be pro-
duced as narrow resonances in e^+e^- annihilation. However, the virtual
exchanges of these particles will produce measurable effects in QED
reactions well below the threshold for production. Thus the QED total
cross section for $e^+e^- \rightarrow \mu^+\mu^-$ will be changed by $\Delta\sigma/\sigma = \pm 8E^2/\Lambda_{\pm}^2$ where E is
the beam energy. These particles would also cause deviations from the
QED angular distribution in $e^+e^- \rightarrow e^+e^-$. The present lower limit on the
mass of either particle is 25 GeV. At PEP this could be extended up to
200 GeV.

(11) TACHYONS

Tachyons are particles that travel faster than the speed of light. In order that energy and momentum be real quantities, tachyons must have an imaginary mass (im_o) if they are to obey ordinary relativistic kinematics:

$$E = \frac{im_o c^2}{\sqrt{1-(\frac{u}{c})^2}} = \frac{m_o c^2}{\sqrt{1-(\frac{c}{u})^2}} \quad ,$$

$$p = \frac{im_o u}{\sqrt{1-(\frac{u}{c})^2}} = \frac{m_o u}{\sqrt{1-(\frac{c}{u})^2}} \quad ,$$

where u = velocity of tachyon $(u > c)$.

A tachyon traveling in vacuum loses almost all of its energy (in the form of Cerenkov light emitted perpendicular to its direction of travel) very rapidly, and accelerates to infinite speed. A tachyon can be identified by the observation of Cerenkov light emitted by the tachyon as it travels through an electric field. This technique was employed by Kreisler et al[1,2] in the search for tachyons possibly photoproduced by γ-rays from radiative decays. The same technique can be applied to search for tachyons in storage rings.
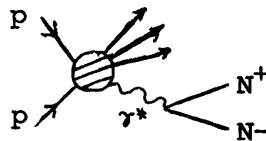
III GENERAL CHARACTERISTICS OF NEW PARTICLES

Let us attempt to summarize the characteristics typical of the new particles, N, detailed in Section II:

A) The most likely direct production mechanism is
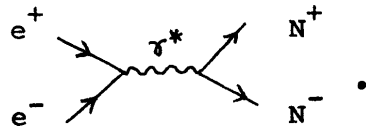
Searches for new particles have been made at FNAL and the ISR, where the process

has not been seen. When the cross section for

$$pp \rightarrow \mu^+ \mu^- X$$

is measured, we will be able to place limits on the cross section for production by virtual photons, which will better determine the rate that can be expected in PEP experiments (see Appendix A).

B) If the $N\bar{N}$ pairs are created well above threshold, and they have no form factor suppression, the production cross section is that of a pointlike Dirac particle of charge q, mass M and spin 1/2,

$$\sigma_{\mu\mu} = \frac{4\pi}{3} \frac{\alpha_q^2}{s} \beta (1 + \frac{M^2}{2s}) \, ,$$

where $\alpha_q = q^2/hc$ and β is the velocity of $N^{\pm}$ in the c.m. frame. Thus, we have

$$\sigma_{N\bar{N}}/\sigma_{\mu\mu} = \frac{q^2}{e^2} \beta (1+M^2/2s)$$

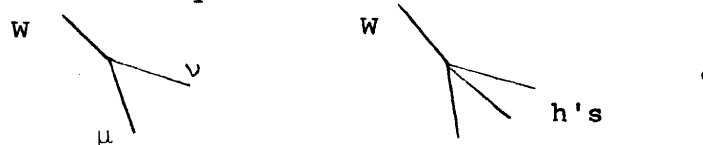for the ratio of the production cross section of N to muon pair production. More generally,

$$\sigma_{N\bar{N}} = \sigma_{\mu\mu} \times TF \times FF \approx \sigma_{\mu\mu},$$

where TF is a threshold factor (≈ 0.7 at $\beta = 0.5$) and FF is the form factor, which we have generally taken as ≈ 1 due to ignorance! This implies high production rates, typically 10^4 new particle events/typical experiment.

C) The decay modes of the new particles determine their experimental signatures and the characterisitics of the detectors built to search for them. We tabulate here a summary of new particle signatures abstracted from Section II, and note the requirements each signature places on a detector.

New Particle Signature	Detector Characteristics
1) Acoplanar $\mu\mu$,ee,μe pairs	μ,e identification and direction
2) 1 observable lepton + hadron	1)
3) 1 observable lepton + "V"	1) + pattern recognition
4) missing $P_\perp$	Calorimetry (including absorption of n and K_L) or <u>Full</u> Magnetic Analysis
5) Massive Colinear pairs	1) + TOF, p, dE/dX
6) Photon Blob	1)
7) 2 Colinear leptons	1) + bump in $\sigma(E_0)$
8) Bump in $\sigma(m^*,MM)$	Full Magnetic Analysis

476

D) The decay mode most susceptible to experimental investigation is that which includes one observable lepton (μ or e). At PEP, pair production and subsequent leptonic decay yields the classic lepton-lepton ($\ell\ell$) signature, or if only one new particle decays leptonically, a lepton-hadron (ℓh) signature. Both of these signatures include neutrinos and therefore missing transverse momentum ($P_\perp$). The rates for these signatures are determined by the ratio of leptonic to hadronic decays:

As discussed in Section IIA, this ratio can be estimated through our knowledge of R, the ratio of rates for

Thus, $\Gamma(N \to \ell\text{'s})/\Gamma(N \to h\text{'s}) \sim \left.\dfrac{1}{R}\right|_{S = \frac{m_N}{2}} \geq \dfrac{1}{10}$,

if we consider pair production of new particles of the highest mass ($m_N \sim 10$ GeV/c^2) accessible at PEP.

We therefore expect a strong suppression of the initially high pair production rates due to the branching ratio:

$$\sigma_{\ell\ell} \sim \frac{1}{R^2}\, \sigma_{N\bar{N}} \sim \frac{1}{100}\, \sigma_{N\bar{N}} \, ,$$

$$\sigma_{\ell h} \sim \frac{1}{R}\, \sigma_{N\bar{N}} \sim \frac{1}{10}\, \sigma_{N\bar{N}} \, .$$

If we ignore the threshold and form factor terms, 100 events with a lepton-lepton and 1000 events with the lepton-hadron signature might be expected in a typical experiment.

IV BACKGROUND IN THE SEARCH FOR LEPTON-LEPTON PAIR AND LEPTON-HADRON SIGNATURES

In the detection of new particles characterized by the presence of a pair of high energy leptons or a lepton plus hadrons there is a source of background associated with the large cross section for hadron production. This background is due to charged pion decay into muons and to conversion of photons from neutral pion decay. Another background is caused by misidentification of a pion as an electron or muon. Two-photon collisions can also produce slightly acoplanar $\mu\mu$ or ee pairs, but not μe pairs.

Pion Decay in Flight

We consider a search for new particles produced at the highest possible mass ($M_N > 10$ GeV). The decay lepton will have momentum 5 GeV/c or higher. Therefore we will concentrate our study of the background on pions with $p \geq 5$ GeV/c decaying into leptons.

Several detectors discussed at the summer study have hadron calorimeters within a distance of 0.75 meters of the interaction region. In addition, we assume that the pion must decay within 1.5 mean absorption lengths (25 cm of Fe or Pb) in the calorimeter. The probability for a 5 GeV/c pion to decay within 1 meter is

$$L/\beta\gamma c\tau = 1 \text{ m}/(50 \times 7.8 \text{ m}) = 0.35\% \text{ .}$$

Using the present data from SPEAR, and scaling to PEP energies (see Figure 3) we obtain the cross section for producing a hadron with $p > 5$ GeV/c ($x > 0.3$) :
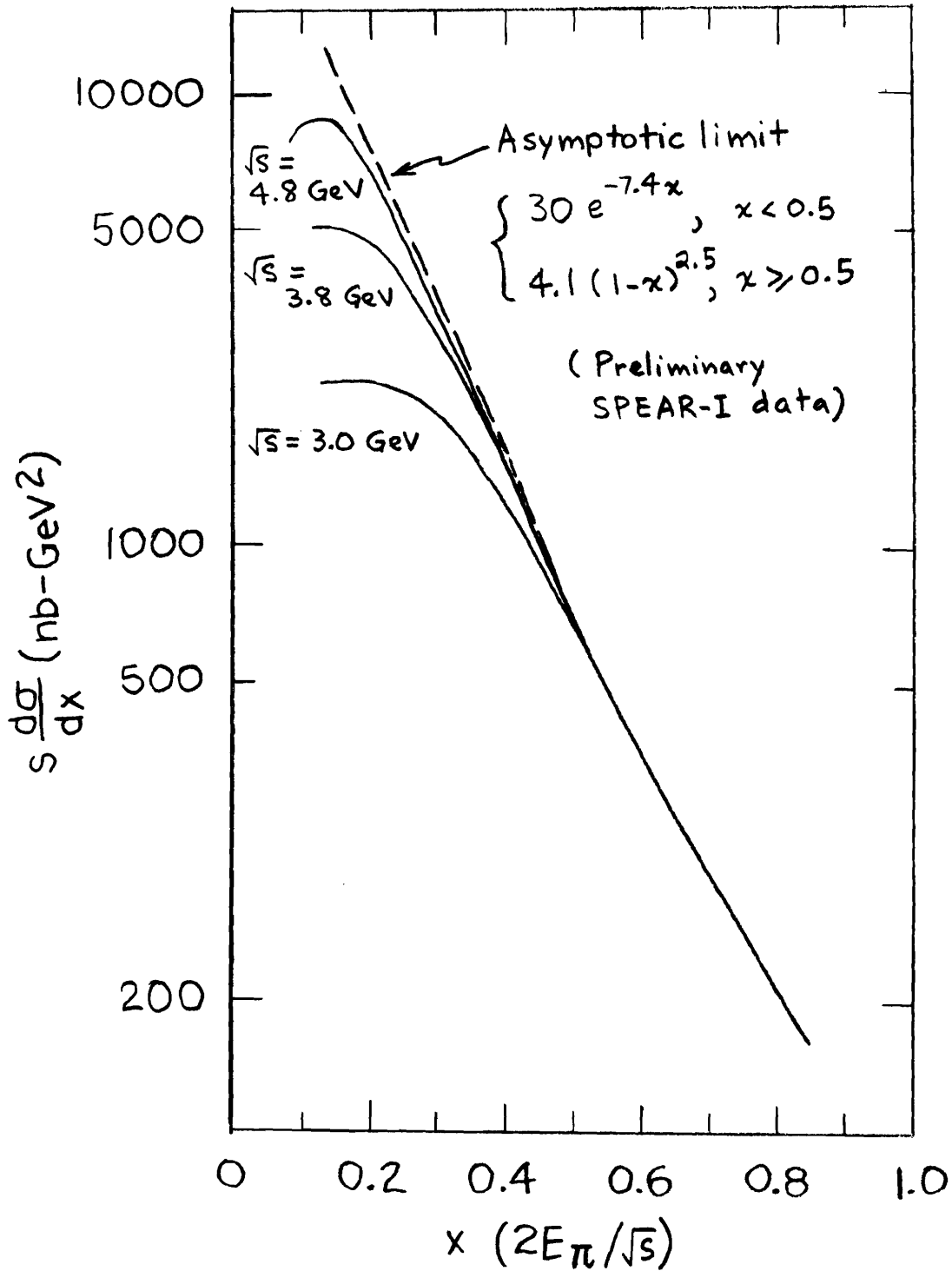
478

Fig. 3

$$\sigma_{\pi > 5 \text{ GeV}} = 0.20 \text{ nb.}$$

This can be compared with the μ-pair cross section at PEP:

$$\sigma(e^+ e^- \to \mu^+ \mu^-) = \frac{84 \text{nb}}{s} = \frac{84}{900} = 0.09 \text{ nb.}$$

Hence

$$\sigma_{\pi > 5 \text{ GeV}} \approx 2\sigma_{\mu\mu}$$

and the cross section for observing a muon coming from a pion decay can be written in the form

$$\sigma_{\mu X} = \text{Production Cross Section} \times \text{Decay Probability},$$

$$\sigma_{\mu X} = (2 \times 0.35\%)\sigma_{\mu\mu} = 0.70 \times 10^{-2} \sigma_{\mu\mu}.$$

Dalitz Pairs and External Photon Conversion

Neutral pions whose photons are converted produce background for the electron signature. Here a 10 GeV π^0 will produce a 5 GeV photon, whose conversion electrons emerge with 0^0 opening angle to mimic one electron. Assuming that the number of neutral pions produced is equal to the charged pion yield, and again scaling from SPEAR to PEP, we find the cross section for inclusive production of a pion with energy >10 GeV is $\sigma_{\pi > 10 \text{ GeV}} = 0.2\sigma_{\mu\mu}$. The pion Dalitz decay probability is 1.2%. The probability of converting one photon in the wall of the beam pipe is pipe thickness/$L_{\text{Rad}} \sim 1$ mm/18 mm $= 5 \times 10^{-2}$. Therefore we get a background

480

$$\sigma_{eX} = (0.2 \times 6) \times 10^{-2}\sigma_{\mu\mu} = 1.2 \times 10^{-2}\sigma_{\mu\mu},$$

which is a factor of 2 larger than the muon background. This background can be reduced substantially by having a magnetic field and detecting the presence of an electron-positron pair by separating them.

Muon-Pion Separation

Another source of background is due to hadron penetration of the absorber that discriminates muons from hadrons. One needs 6 absorption lengths to reduce this source of background to the same level as that from $\pi-\mu$ decays ($e^{-6} = 0.25\%$). Hence one needs about 1 meter of iron or lead to obtain good muon-hadron separation. The energy threshold for this thickness is 1 GeV. For energies above this, good rejection against pions is obtained by requiring no large deposition of energy in the iron. A simple counter after the iron is not sufficient to distinguish between π's and μ's. Sampling is necessary since low energy hadrons can emerge after 6 interactions lengths even though the hadronic shower is almost totally contained.[+] However, since the amount of material required for $\mu-\pi$ separation is also the amount necessary to fully contain the energy of the shower, the muon identifier can simultaneously be a hadron calorimeter if made of active material.

[+] J. Engler et al, NIM <u>106</u>, 189 (1973)

Electron-Pion Separation

Charged pions and electrons shower differently in high Z materials such as lead. However, through charge exchange or δ-ray production pions can simulate electrons. By sampling the energy deposited at different depths of a shower, a high rejection ratio can be achieved against pion contamination in the identification of electrons. Momentum analyzed pions above 10 GeV/c can be distinguished from electrons with a rejection factor of $>10^4$ by sampling the first and second halves of the shower separately.[+] Events populate a plot of energy deposited in the first half vs that deposited in the second half as follows:
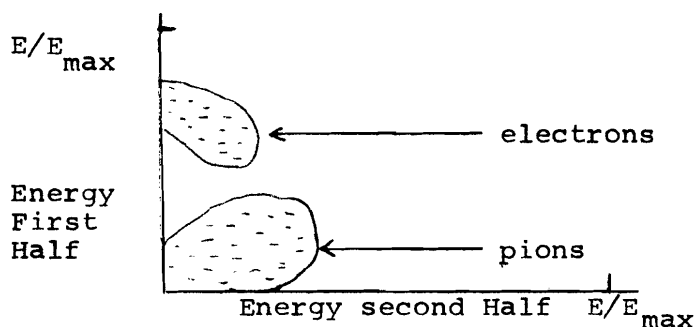
The rejection factor is worse for a mixture of pions and electrons with unknown momentum because high energy π's simulate low energy e's. Since high energy π production is severely suppressed one expects a rejection factor better than 10^2 un-

---

[+]D. C. Cheng, Private Communication; P. Limon, Private Communication.

der these conditions especially if one samples the shower 3 to 4 times and requires a transition curve characteristic of an electron shower. Thus the probability that a π^+ simulates an electron in a shower counter is of the same order of magnitude as the probability for a photon from a π^0 to convert.

Signal-to-Noise Ratio

To calculate a signal-to-noise ratio we need the production cross section for the new particles and their decay branching ratio into leptons as compared to hadrons, neither of which is well known. Consider electromagnetic pair production above threshold

$$\sigma(e^+ e^- \to N\bar{N}) = \sigma_{\mu\mu} \times TF \times FF \sim \sigma_{\mu\mu}$$

In general, we expect

$$\frac{\Gamma(N \to \text{hadrons})}{\Gamma(N \to \text{leptons})} \approx \frac{\sigma(e^+ e^- \to \text{hadrons})}{\sigma_{\mu\mu}} = R \quad (\text{at } \sqrt{s} \approx M_N/2) \, .$$

T F is the threshold factor, which can be quite small as in the case of $W^+ W^-$ production (0.1 for $M_W \approx 0.9 \, E_0$). In general, though, T F $\sim$ 0.7 if $\beta \sim 0.5$. From SPEAR,

$$R \approx 5 \text{ for } M_N \approx 10 \text{ GeV.}$$

We then obtain for single lepton detection

$$\frac{\text{signal}}{\text{noise}} = \frac{e^+ e^- \to N\bar{N} \to \ell + \text{hadrons}}{e^+ e^- \to \text{hadrons} + (\pi \to \ell)} = \frac{1/R \times TF}{0.7 \times 10^{-2}}$$

$$= \frac{0.7/5}{0.7} \times 10^2 \approx 20/1 \quad .$$

In searching for the pure lepton pair signature, unaccompanied by any other charged particles, rejection of events with more than 2 charged particles or with any gamma rays in a large solid angle detector will greatly increase the signal-to-noise ratio.

(D) BACKGROUND FROM QED PROCESSES

Single photon exchange produces $\mu\mu$ and ee pairs that are collinear. These processes provide an excellent calibration for the shower counters and muon identifiers at detectors used in particle searches sensitive to final-state leptons. Radiative corrections to these processes effectively shift the center of mass of the collision, thereby destroying collinearity of the final lepton pair, but preserving coplanarity. Therefore these processes do not produce background to the acoplanar $\ell\ell$ new particle signature.

Two photon collision processes, however, can produce acoplanar $\mu\mu$ or ee pairs via diagrams like
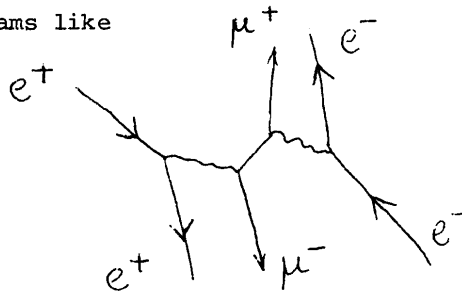
where the photons are nearly real and the initial e^+ and e^- go down the beam pipe. This background is both calculable and can be strongly suppressed by cuts both on the energy of the observed lepton pair and on their acoplanarity; e.g., for a requirement that both leptons exceed 1 GeV, the rate of two photon events is $\sim \sigma_{\mu\mu}$.[†] Further, these events are nearly all within $5°$ of coplanarity. The rate of two photon collision events decreases as $1/S$ relative to $\sigma_{\mu\mu}$, so that a threshold of 5 GeV has a background rate $\sim 4 \times 10^{-2} \sigma_{\mu\mu}$ before any cuts on coplanarity. Indeed, this process may provide a very useful calibration tool since the $\mu\mu$ and ee pairs are produced at all energies -- as contrasted with the fixed energy of single photon events. Measurements by an internal magnet detector can be correlated with energy and range measurements of μ's and e's. We stress that this process does not contaminate the general new particle signature of a μe pair in the final state.

[†] H. Terazawa, Rev. Mod. Phys. 45, 615 (1973).

V TYPICAL NEW PARTICLE DETECTORS

In this section we discuss several typical detectors opti-
mized to search for new particles. Their characteristics are
described with the goal of determining guidelines for the design
of the PEP experimental areas.

All the detectors share certain salient features which we
outline here:

1) Interaction Region. Highest possible luminosity is re-
quested, since the most characteristic signature, μe, is sup-
pressed by the leptonic branching fraction to perhaps 100 events
into 4π. The vacuum pipe must be thin to prevent background
and to avoid particle misidentification due to photon conversion
and δ-ray production. The beam pipe should narrow to a diameter
as small as possible around the interaction region to allow high-
est efficiency for identifying short-lived "V's".

A thin ceramic pipe may be required for effective streamer
chamber operation. A superconducting pipe may be necessary if
a transverse field is used near the pipe. This prevents the field
from sweeping low energy background into the detector.

We visualize the next elements of the schematic detector as
spherical shells concentric about the interaction region. Near
4π geometry is required by the low rates we expect for new phe-
nomena.

2) Pattern Recognition and Track Detection Device. This
element of the schematic detector might be a) a streamer cham-
ber with its unexcelled pattern recognition capabilities,

486

b) drift chambers if events are characterized by low multipli-
cities or c) a calorimeter if the high multiplicities suggested
by the thermodynamic model prevail. This option avoids pattern
recognition; instead, it measures the resultant vector momenta[†]
for each of these components of the final state: the neutral
electromagnetic, the charged electromagentic, the charged had-
ronic, and the neutral hadronic $(K_s^0$ and n).

This region may have magnetic analysis. - four simple options
exist: transverse (or split) field, longitudinal field (a
toroidal field) or no field.

The size of this volume is limited to $\sim$0.7 m radius by two
considerations: a) π/μ separation requires absorber as close
as possible to the interaction region to prevent π decay in flight,
and b) the mass and cost of any calorimeter or muon identifier
outside this volume grows as R^3.

3) Electron/Photon Identifier. The next spherical shell
of the ideal detector is $\sim$12 radiation length ($\sim$15 cm) of elec-
tron identifier (Pb Glass, Pb-Scintillator or Pb-Argon). Samp-
ling of the shower energy is performed $\gtrsim$ 3 times to discriminate
between π's and e's. This unit could also record dE/dX and
time-of-flight information useful in identifying particles oth-
er than electrons.

[†]See Report on Calorimeters by J. Marx, L. Sulak and D. Yount in
this study.

4) Muon Identifier   and/or Hadron Calorimeter. The last layer of detector has a thickness of ~6 absorption lengths (~ 1 m iron) necessary for i) separation of muons from pions by absorption of the π's; $\gtrsim 3$ dE/dx samplings are necessary to distinguish π's from μ's. ii) the iron may be magnetized (if μ momentum is desired) in which case position location devices are required, iii) six L_{abs} are also required to totally contain a hadronic shower if calorimetry is done in this layer. The sampling may be crude if one wishes merely to veto hadronic events, or fine grained if missing transverse momentum is being measured.

We proceed to describe several realizations of this schematic detector.

(A) SMALL SOLENOID MAGNETIC DETECTOR

Physics Goals

1. New particle searches through good muon and electron identification; missing energy and transverse momentum; thresholds and bumps in partial cross sections; mass measurement of long-lived particles; K^0_S and Λ abundance .

2. Hadron Production - $\sigma_{TOT}(e^+e^- \rightarrow$ hadrons); charged and neutral multiplicities; charged particle spectrum at low momentum; γ, π^0 spectra at high momenta .

3. QED Experiments - $e^+e^- \rightarrow e^+e^-$, $\mu^+\mu^-$, $\gamma\gamma$; virtual Compton scattering $\gamma^*e \rightarrow \gamma e$.

Description

This detector (Fig 4a, b) consists of three main parts:

1) A solenoidal magnet and cylindrical drift chambers for the detection and momentum analysis of charged particles.

2) Active converters, proportional chambers and shower counters for photon detection and energy measurement as well as electron identification.

3) Iron interleaved with scintillation counters and followed by drift chambers for the detection of n's and K^0_L's, rough calorimetry and muon identification.

Going outward from the interaction region we have:

1) The beam pipe - 6 mil stainless steel.

2) 4 cylindrical drift chambers, 2 gaps each; spatial resolution = ± 0.1 mm in azimuthal coordinate, ± 1 cm in longitudinal coordinate (provided by a delay line near each sense wire). These can be used to provide trigger signals.
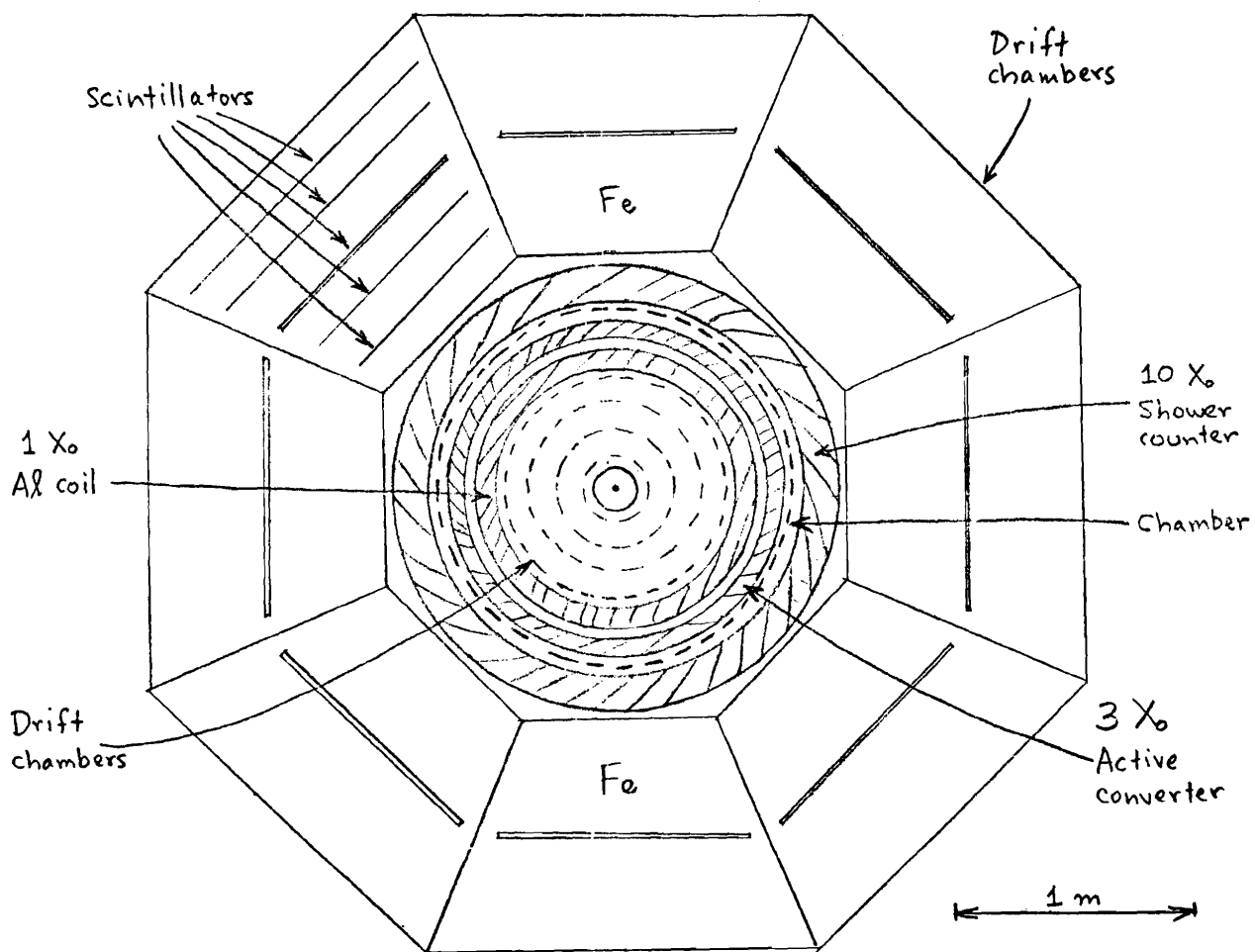
489

Small Solenoid Magnetic Detector (end view)

Scintillators

Drift chambers

Fe

Fe

10 X₀ Shower counter

Chamber

3 X₀ Active converter

1 X₀ Al coil

Drift chambers

1 m

FIGURE 4a

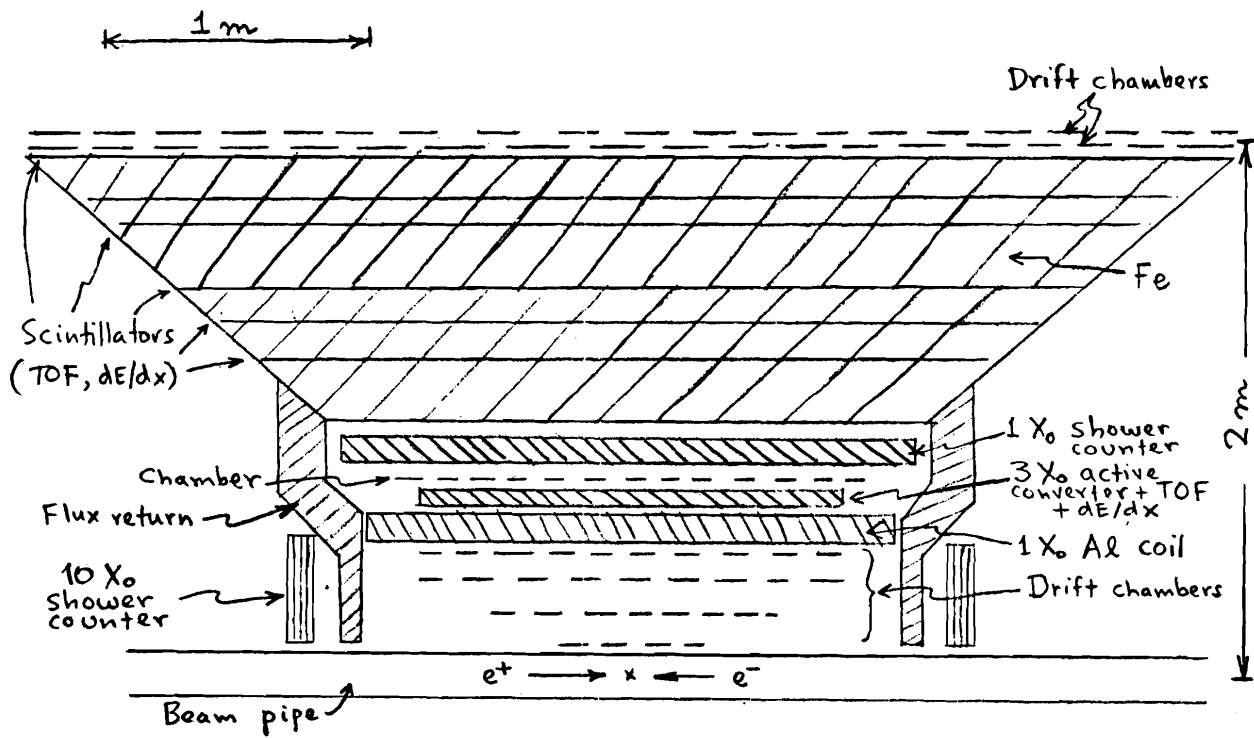Small Solenoid Magnetic Detector (side view)

FIGURE 4b

491

3) Magnet coil - 1 X_o Aluminum. Field at 8 KG; power consumption = 900 KW.

4) Active converter - Pb-scintillator sandwich, 3 X_o thick; 48 units with a phototube on each end. This is used for time-of-flight and dE/dx measurements as well as for photon conversion and shower energy measurements.

5) Proportional chamber - for spatial localization of the photons.

6) Shower counter - Pb-scintillator sandwich, 10 X_o thick. 48 units with a phototube on each end: this is for shower energy measurements.

7) Iron - a total of 5 collision lengths. This is for hadron absorption and calorimetry. It is also used for flux return.

8) Scintillation counters - for time-of-flight and calorimetry.

9) Drift chambers - these measure the direction and location of particles emerging from the iron ·and are used for muon identification.

Miscellaneous components - end cap chambers and shower counters are used to detect charged particles and photons emerging at small angles. Compensating coils are needed to make $\int B \cdot dl = 0$.

Capabilities

1) Solid angle for charged particles with good $\Delta p/p$ = 87% of 4π sr.

    "   "   "   "   "   detection   = $\sim$98% "   "

    "   "   "   photon detection   = 75% "   "

    "   "   " electron and muon identification = 75% "   "

2) $\Delta p/p$ for charged particles = 9% at p = 3 GeV/c and is proportional to p (except at low momenta where multiple scattering effects dominate).

3) $\Delta E/E$ for γ's and e's = $10\%/\sqrt{E}$ (E in GeV).

492

4) Time of flight measurement - can pick out particles with $\beta < 0.5$ at 2σ level (assuming $\sigma = \pm 0.5$ nsec).

5) Electron identification is based on the shower energy measurements in the active converter and shower counter for a particle of <u>known</u> momentum. This provides a pion rejection factor of $\sim 10^{-4}$.

6) Muon identification is based on minimum ionizing signals in the active converter, shower counter, and calorimeter scintillators combined with a final trajectory, as determined in the drift chambers, consistent with multiple scattering for a particle with the measured momentum. Pion rejection is limited to about 10^{-2} (for $p_\pi = 1.5$ GeV/c) due to $\pi \to \mu\nu$ decays in flight.

7) The missing energy and transverse momentum measurement is based on momentum analysis for the charged particles, shower counter energy measurement for the γ's, and calorimetry for the K_L^0's and n's. Assuming 10 $\pi^\pm$'s, each with $p = 1.5$ GeV/c and 20 γ's, each with $E = 0.75$ GeV, in the detector, the total energy (30 GeV) will be measured to ± 0.5 GeV.

(B) SPLIT FIELD DIPOLE MAGNETIC DETECTOR

This detector is designed to search for new particles whose decay can be characterized by the presence of muons, electrons, strange particles, or the absence of a large amount of transverse momentum.

The device utilizes a magnetic detector with field transverse to the beam direction. It has been demonstrated at Adone that a transverse field at the beam pipe has very adverse effects on detection capabilities, since large numbers of low energy particles are swept out of the beam pipe. This device avoids the problem with a split field along the beam line.

A top view of the apparatus is shown in Fig.5 and 6. It consists of four semicircular pancakes (two above and two below the beam line). The two halves of the circular magnet produce a field oriented in opposite directions on each side of the beam pipe. Thus only a low field exists in the region of the beam and no field (by symmetry) in the interaction region. In addition a simple superconducting pipe may be necessary to remove any remaining field. The outer radius of the magnet is 75 cm, and the distance between pole pieces is 1.50 meters. (See Appendix B).

Wire chambers or drift chambers each of height 1.50 meters are placed inside the magnet in the arrangement shown. The solid angle acceptance is 2π for particles that go out the side of the magnet. A larger solid angle is achieved for charged particles whose momentum is measured by the wire chambers but whose trajectories hit the pole pieces.

The chambers consist of 5X chambers and 3Y chambers as shown. Assuming a net spatial resolution of 0.4 mm/plane and a field integral of 2.5 kG meters, we get a momentum and angular resolution

$$\Delta\theta \approx 10^{-3} \text{ rad}$$

$$\frac{\Delta p}{p} = \frac{(\Delta\theta)p}{0.03 \text{ HL}} = \frac{p}{75} \text{ (GeV/c)}$$
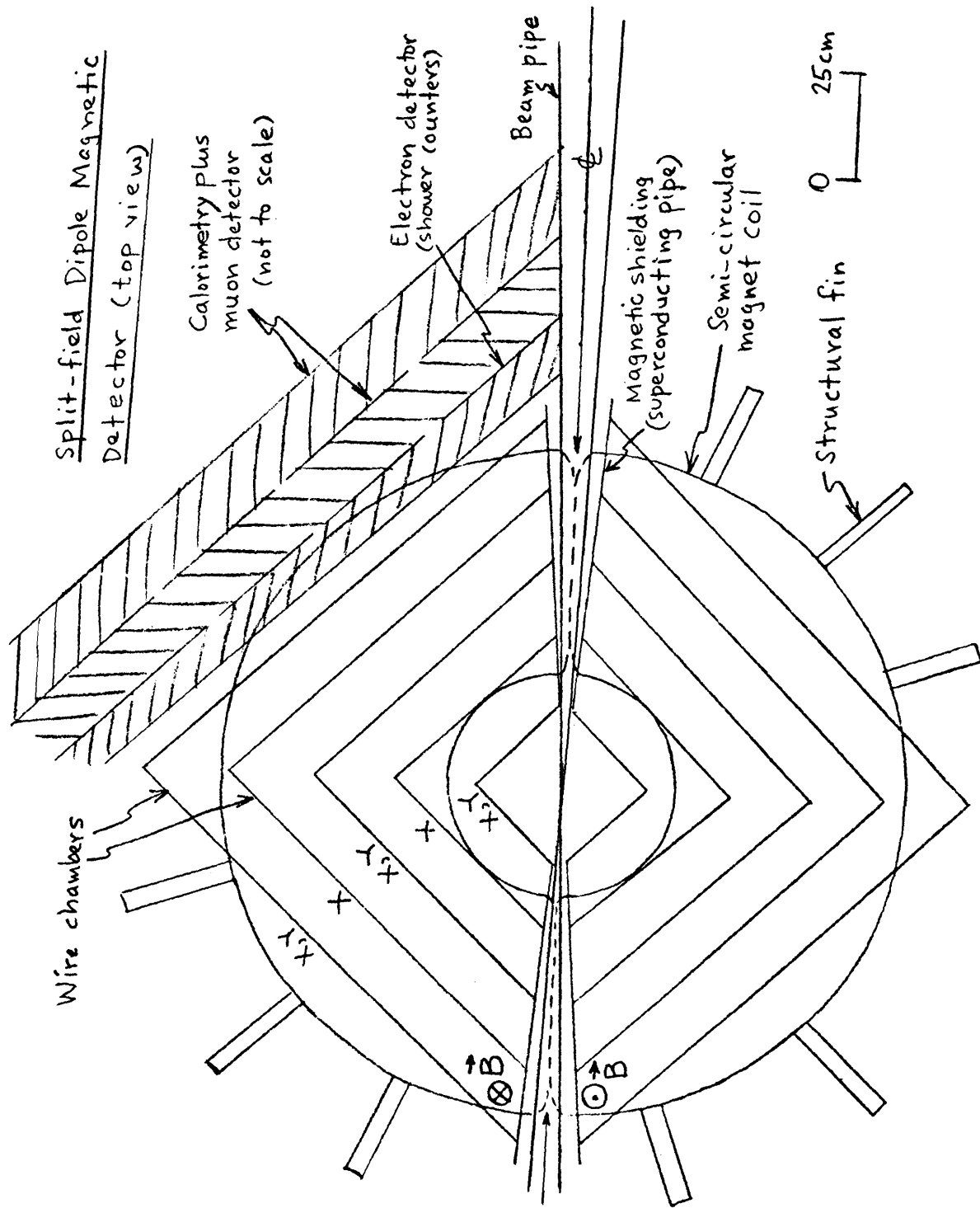
Split-field Dipole Magnetic Detector (top view)

Calorimetry plus muon detector (not to scale)

Electron detector (shower counters)

Beam pipe

Magnetic shielding (superconducting pipe)

Semi-circular magnet coil

Structural fin

25 cm
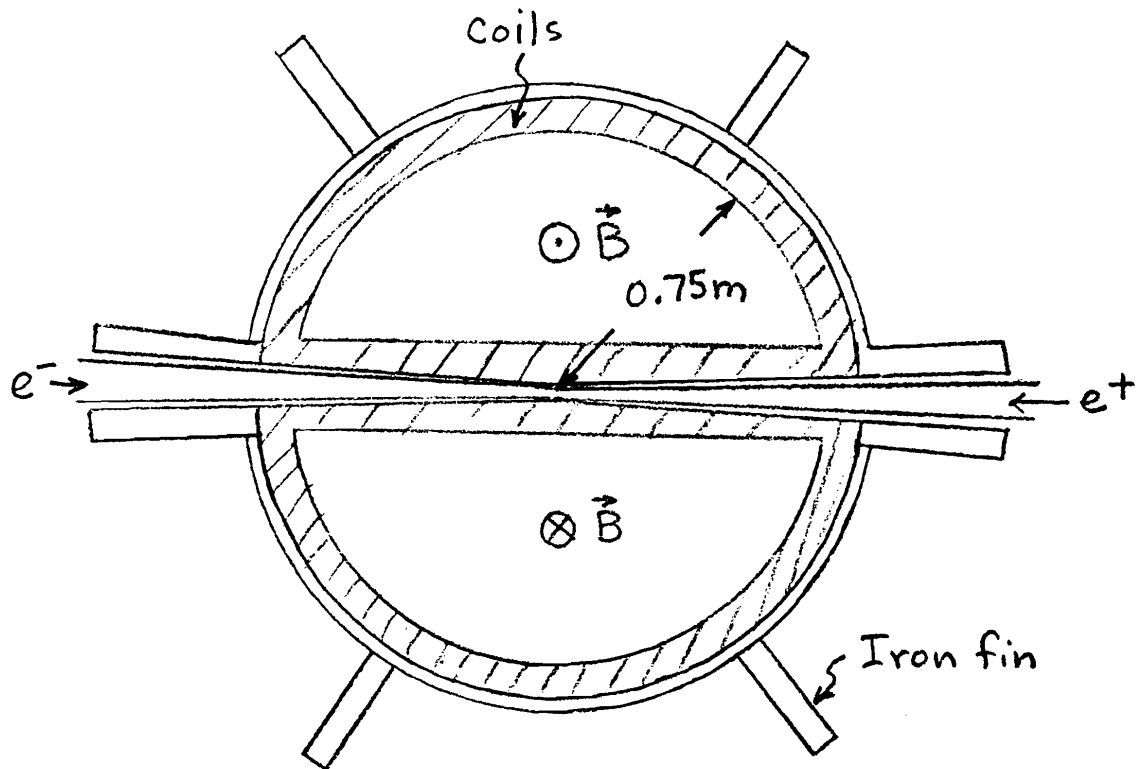
Wire chambers

FIGURE 5

495

Split-field Dipole Magnetic Detector (top view)

FIGURE 6

Since the region between the pancakes is completely open   except for the structural fins shown in Fig. 5 , particle identification devices like lead glass for electrons and gammas, neutral hadrons detectors (calorimeters) and muon filters can be placed in a cylindrical arrangement at a distance of 75 cm from the interaction region. The probability for a 5 GeV/c pion to decay into a muon in that distance is 0.3%. Also the majority of Λ's and K_S's will decay within the radius of the magnet.

This device can be easily used in various experiments which differ from one another by the calorimetric devices placed around the magnet.

The power needed to run this magnet is about one megawatt for a central field of 5 kG. The magnet should be constructed in such a fashion that the pole pieces can be easily separated by lifting the top pole piece for access to the chambers inside the magnet. This, as well as the calorimeters, requires a crane.

A typical calorimeter is shown in Fig. 7 . It consists of a shower detector made up of lead scintillator sandwich. The light from the various scintillators at a given radius would be added before going to a phototube. Phototubes at the top and bottom obtain z position information by time of flight. A calorimeter to detect hadrons consists of 4" of steel sandwiched with 6" of liquid scintillator cells. Again the phototubes will alternate top and bottom to obtain z position measurement by time of flight.

The advantages of this type of detector include simple x,y determination of position plus the ready accessibility to the interior of the detector. One disadvantage is the quadrupole nature of the magnetic field near the central plane between the magnet halves.
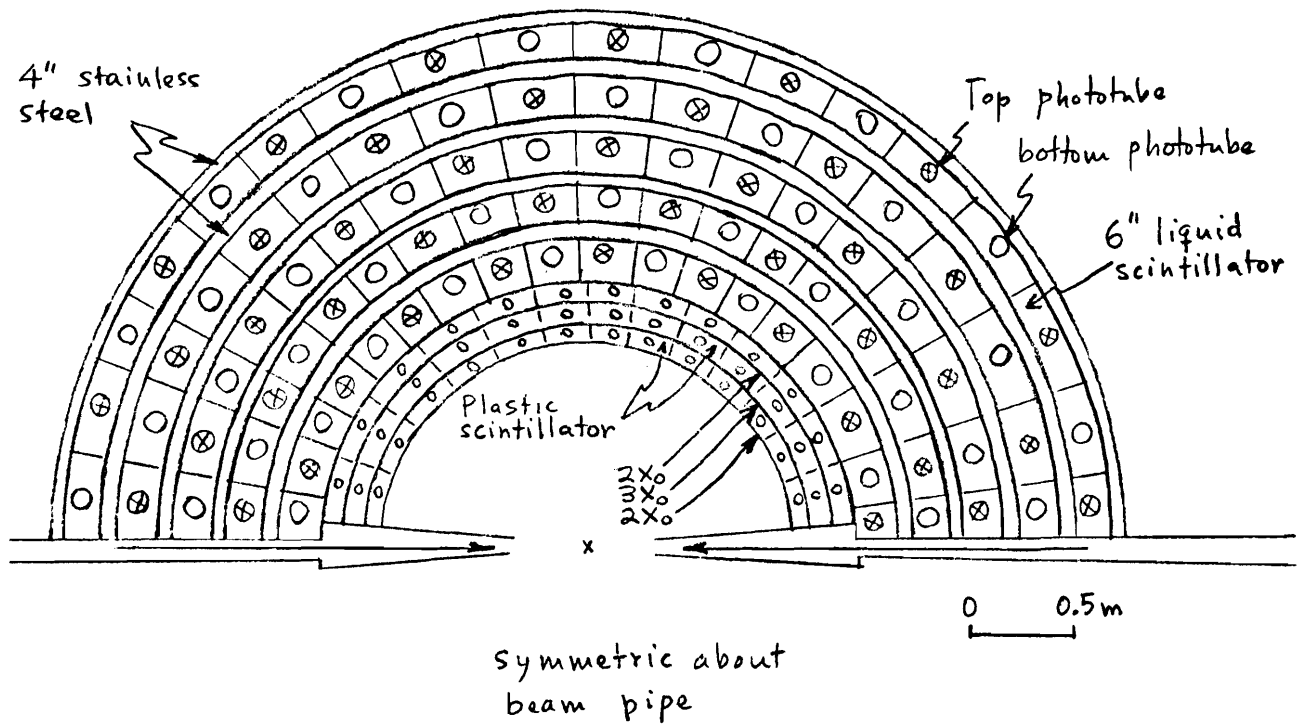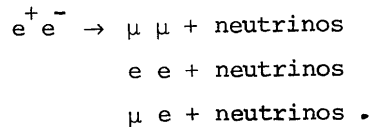
Calorimeter

FIGURE 7.

(C) MUON-ELECTRON MAGNETIC DETECTOR

This detector is designed to study heavy lepton or W boson production by detecting two leptons in the final state:

$$e^+ e^- \rightarrow \mu \; \mu + neutrinos$$
$$e \; e + neutrinos$$
$$\mu \; e + neutrinos \; .$$

The rejection efficiency for other particles faking two leptons is large $(\sim 10^4)$.

The signature for heavy lepton or W production is a pair of leptons with a large missing momentum vector that does not point down the beam pipe. The solid angle coverage of the detector is 2π steradians; electron momentum resolution

$$= \frac{\pm \; 10\%}{\sqrt{E \; (GeV)}} \quad ;$$

muon momentum resolution = $\pm$ 20%.

The detector consists of three major parts, each of which surrounds the beam pipe in octants as shown in Fig. 8 :

(1) Inner cell of scintillation counters and spark chambers.

Eight scintillator pairs form the trigger for each octant. Time of flight between the crossing point and the outer scintillator, together with range or momentum measured in subsequent parts of the apparatus, can be used to measure the mass of a long-lived heavy lepton. A mass measurement can be achieved if $\beta_{lepton} \lesssim 0.7$.

Three sets of U-V spark chambers measure charged particle track positions. By reading wires at both ends of the chamber large stereo angles can be achieved. With wire spacing of 1 mm, the angular resolution will be $\sim \pm$ 10 mrad.

(2) Shower detector and electron calorimeter.

The shower detector is designed to identify electrons and separate them from hadrons. This is achieved by sampling the electromagnetic shower in a lead, liquid scintillator detector at several depths and comparing these with the total energy deposited in the calorimeter. Some parameters of the calorimeter are

number of cells sampled	$8 \times 40 = 320$
thickness	16 radiation lengths
weight of lead	9 metric tons
weight of scintillator	3 metric tons
number of phototubes	640
energy resolution	$\sim 10\% / \sqrt{E(GeV)}$
hadron rejection factor	20 - 50
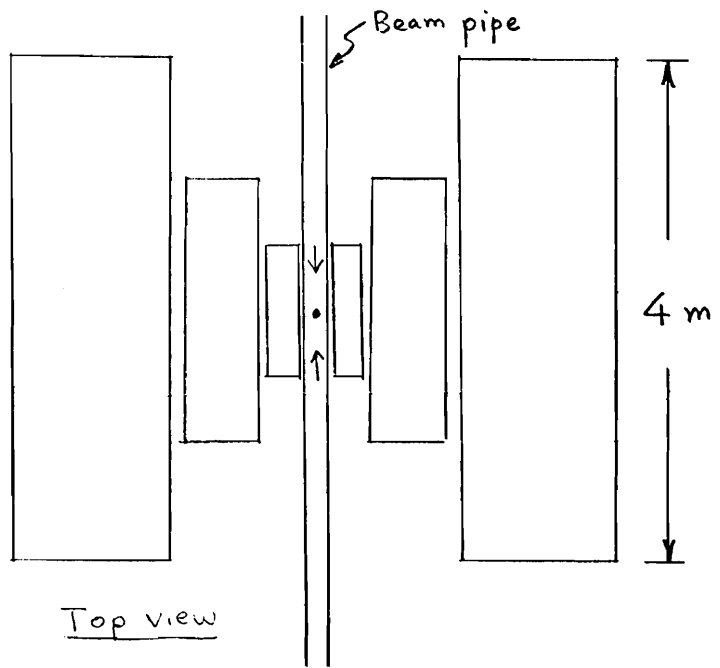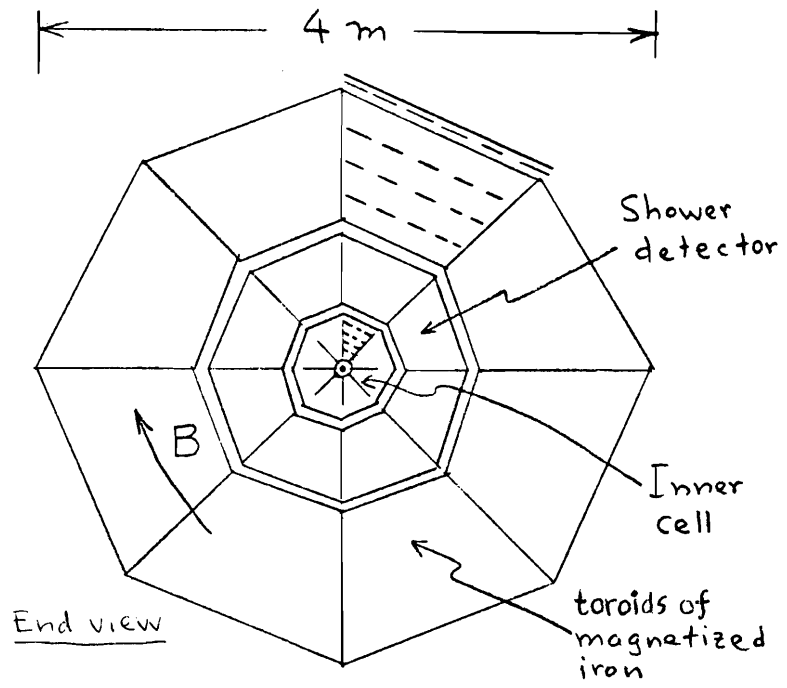
Muon—Electron Magnetic Detector

FIGURE 8

500

(3) Muon spectrometer.

The muon spectrometer is designed for muon identification and momentum measurement. It consists of toroids of magnetized iron sandwiched between five planes of spark chambers. The spectrometer parameters are

length	3.5 m
ID	2.0 m
OD	4.0 m
weight	375 metric tons
B	15 kG
Current	7500 amperes turns/meter of toroid
spark chamber wire spacing	2 mm
area of spark chamber U-V	240 m^2
number of wires	96,000 wires
muon momentum resolution	20%
hadron rejection ratio	100 - 200
scintillation counters	64 m^2
phototubes	32

(D) <u>MUON-ELECTRON NON-MAGNETIC DETECTOR</u>

This detector is designed to search for new particles whose signatures are the presence of 2 or more non-colinear leptons (ee, eμ, μμ, eeγ, etc.) fractionally charged particles, or massive quasi-stable pairs of colinear particles. Simultaneously, this detector can measure QED processes, the total hadronic cross-section, and semi-inclusive π^0 processes, $\frac{d\sigma}{dx}$ ($e^+e^- \rightarrow n\pi^0 + X$).

The charged particle directions are detected by 4 sets of cylindrical drift chambers (with cathode readout of the azimuthal track direction) plus a pair of end cap chambers, covering over 99% of the total solid angle (see Fig.9). Immediately after the drift chamber is a set of scintillation counters used to detect colinear massive pairs of fractionally charged particles using energy loss ($\frac{dE}{dx}$) and time-of-flight techniques.

Surrounding the position detectors, a set of shower counters identify electrons over 95% of the total solid angle. The shower detector would probably be a liquid argon detector, having 4 separate pulse height samplings along the depth of the shower to separate π's from e's. The most severe background in electron identification comes from Dalitz pairs (1.2% per decay), and gamma conversions in the beam pipe.

Outside of the shower counters, five absorption lengths (85 cm) of iron, with $\frac{dE}{dx}$ scintillation counters interspersed between layers of iron, form a muon identifier.

Muons can be separated from hadrons to better than 1% by requiring that all $\frac{dE}{dx}$ counters yield a signal compatible with that of a minimum ionizing track. An unavoidable background comes from $\pi^{\pm}$ decay into $\mu^{\pm}\nu$; e.g. the probability for 5 GeV/c pions to decay before encountering the shower counter is 0.1%.

Muon-Electron Non-magnetic Detector
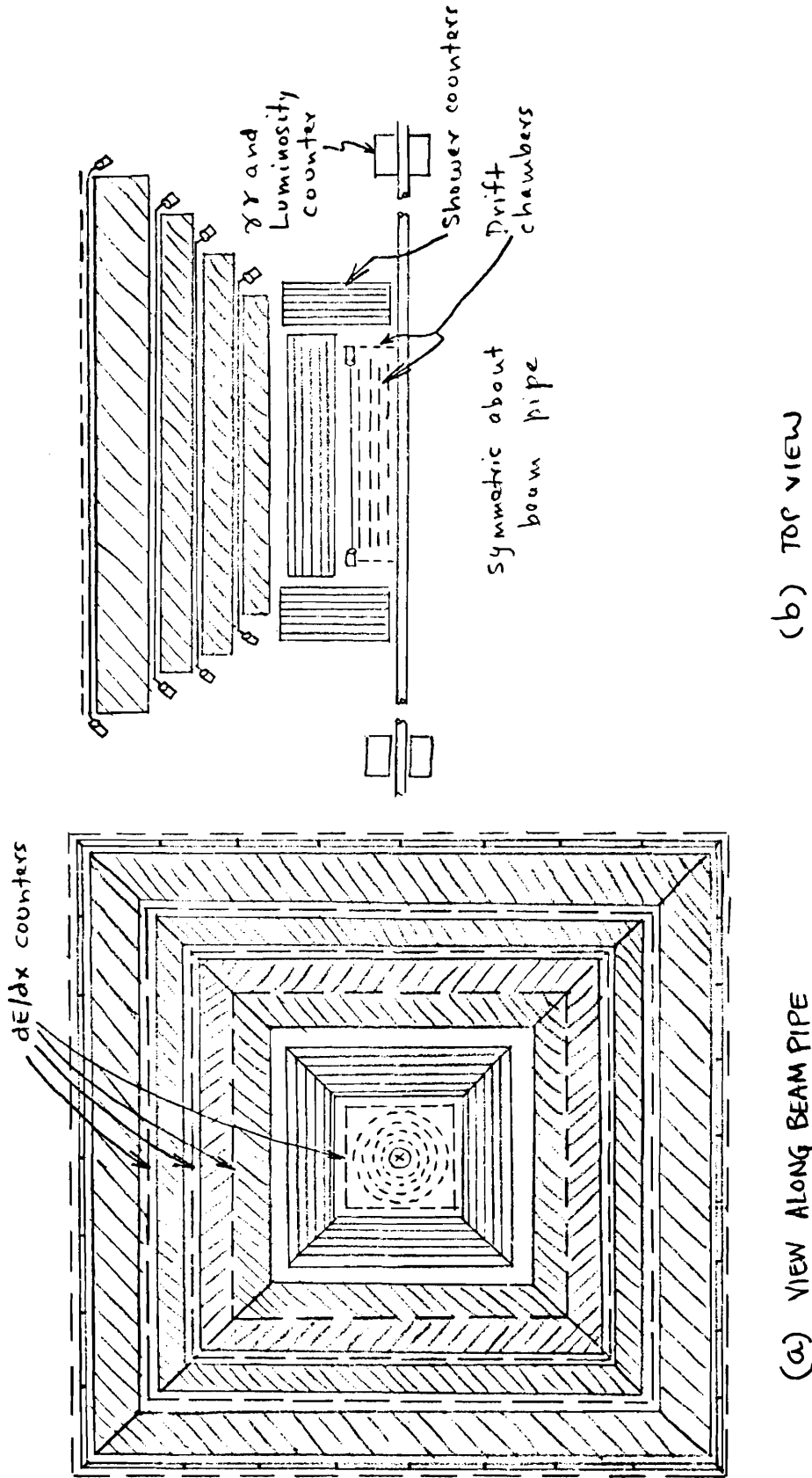
(a) VIEW ALONG BEAM PIPE

(b) TOP VIEW

FIGURE 9

503

(E) CHARMED PARTICLE DETECTOR

The general signature for pair production of charmed hadrons is a final state including one or more strange particles and possibly a muon or lepton if one of the charmed particles decays leptonically. Two hadronic decays with only one having a strange particle (e.g. apparent violation of strangeness) appear to be a very difficult signature. (This signature could be mimicked very easily by associated production of a K_L^O and its subsequent escape.

A cleaner signature involves a strange particle associated with a lepton. Important characteristics of a charm particle detector for this mode are

(1) Good muon and electron identification

(2) A good resolution for identifying "V's"

(3) Good π^O identification (useful in detecting Σ^+ decay.)

A streamer chamber surrounding the interaction region (see Fig. 10) especially if outfitted with external electron and external muon identification, seems to be an ideal detector due to the excellent pattern recognition ability of this device.

Further, ionization measurements are useful for heavy particle identification and time-of-flight measures β for $p < 800$ MeV/c. Momentum resolution is $\sim 9\%$ at 15 GeV/c (B=2 Kg).

Options that can be added to the bare chamber to enhance the ability to identify new particles are

1) Transparent drift chamber end caps

2) γ detectors on open sides of the magnet

3) Calorimeter γ and μ identification on closed sides of magnet

4) A small bore beam pipe to catch "V's"

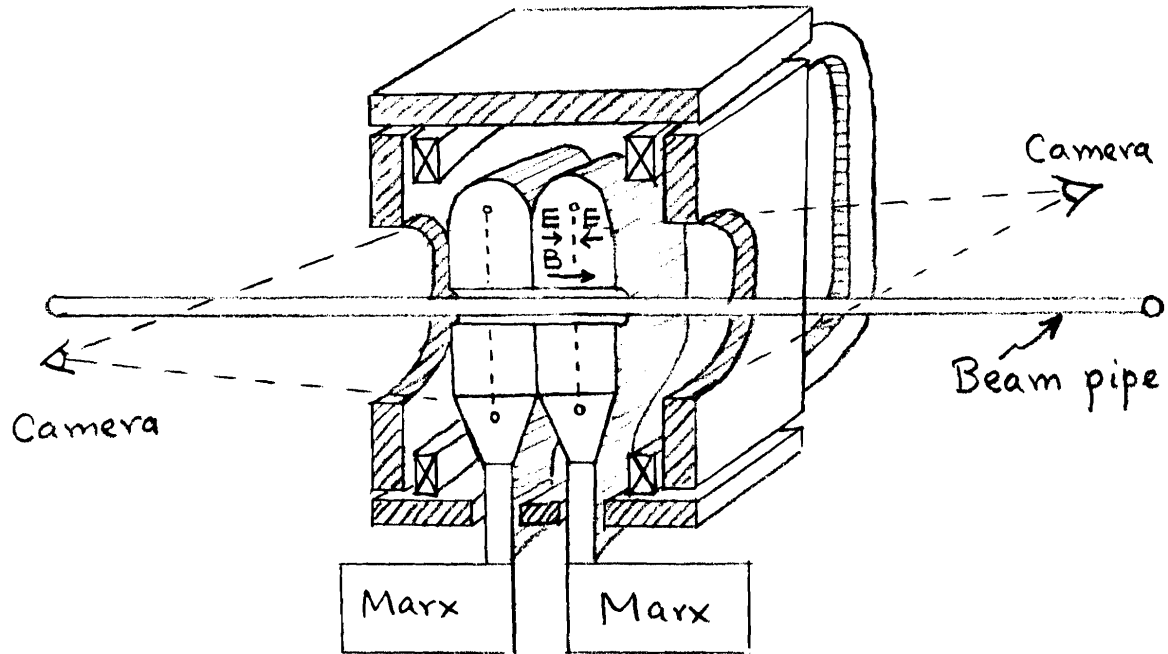5) PbO_2 inside the chamber for γ and e identification

Streamer Chamber

FIGURE 10

6) MWPC's between a metal beam pipe and the electrostatic shield (if necessary) to measure initial track positions.

We encourage the development of this device.

For a nonvisual search it appears that a magnet is not necessary to measure the inclusive strange particle production, or the presence of strange particles correlated with leptons. It also seems that a detector with a rectangular coordinate system would pick up V's with higher efficiency than a solenoidal geometry, even though it subtends less solid angle. The ability of the present solenoid detector at SPEAR to reconstruct V's is marginal due to its inability to measure accurately both x and y coordinates.

We propose a non-magnetic detector with 90° stereo. Such a device could be a box around the interaction region as shown in Fig.11, surrounded by electron shower counters and calorimeters for hadron-muon identification. For a search experiment, it may not be necessary to have good calorimetry, but only enough to positively identify muons.

The probability of picking up V's as decays of strange particles is much better than for their charged counterparts. The K^{+} lifetime allows it to leave the detector without decaying a very large fraction of the time. On the other hand, the vertex of $\Sigma^{\pm}$ decays will often be inside the beam pipe. One would like to construct a thin walled spherical beam pipe around the interaction region, to minimize interactions and multiple scatter-

Charmed Particle Detector

Symmetric on
either side of
interaction region

Shower counter

Drift or proportional
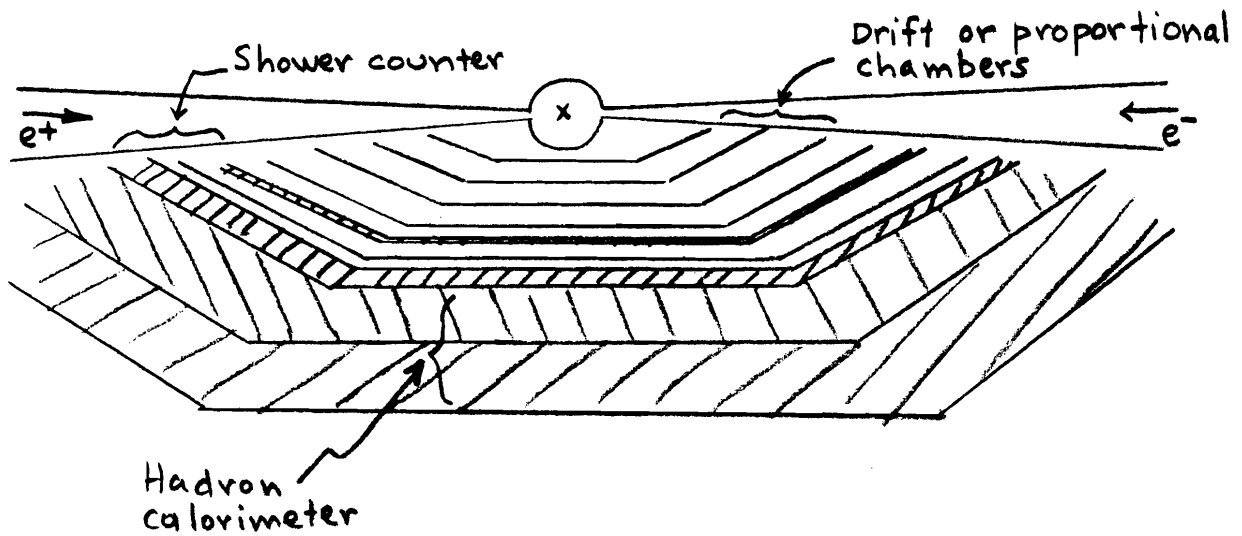chambers

e^+ x e^-

Hadron
calorimeter

FIGURE 11

ing in the walls and to catch V's as close as possible to the inter-
action region.

Since the general rate is low, a loose two particle trigger
would suffice. If proportional wire planes were used, a "V" trig-
ger could be set up.

The "time projector detector" of D. Nygren, without a magnet,
has sufficient resolution ($\sim$ .3 to .5mm) to pick out strange par-
ticle V's, and has the advantage of 3-dimensional information, so
that there are no pairing ambiguities.

VI   CONCLUSION - BUILD PEP!!

... with highest possible luminosity. Significant new
particle searches can be performed at PEP with only minimal
requirements on the length of the interaction region and on
the beam pipe at the interaction region.

TABLES 1-11

SUMMARY OF NEW PARTICLE INFORMATION

(1) Heavy leptons - excited, sequential, gauge theory, and quasi-stable heavy leptons

(2) Charged Intermediate Vector Bosons

(3) Charmed Hadrons

(4) Resonances

(5) Quarks

(6) Gluons

(7) Monopoles

(8) Higgs Scalers

(9) Neutral Intermediate Bosons

(10) Lee-Wick Particles

(11) Tachyons

The following abbreviations are used in the tables:

ℓ = either e or μ
h = hadron
MM = missing mass
M = new particle mass
m* = invariant mass
COP = coplanar
ACP = acoplanar
COL = colinear
β = velocity of new particle in center of mass system
R = $\sigma(e^+e^- \to hadrons)/\sigma(e^+e^- \to \mu^+\mu^-)$
FF = form factor

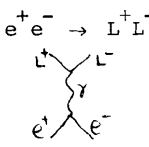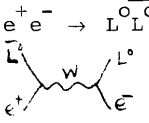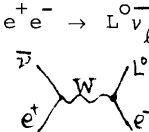| Particle	Production Mechanism	Rate per $\left\{\begin{matrix}10^{38}\ cm^2\\10^4\ \mu^+\mu^-\end{matrix}\right.$	Decay Modes/ Branching Ratios	Experimental Signatures	Present Limits	PEP Limit
(1) HEAVY LEPTONS [1]						
(A) Excited leptons $\ell^-, \ell^{*-}\ldots,$ $\nu_\ell, \nu_\ell^* \ldots$	$e^+e^- \to \ell^{*+}\ell^{*-}$ $\ell^{*+}\ell^-$ $\ell^+\ell^{*-}$	$10^{-4} \times \left(\frac{3\beta-\beta^3}{2}\right)$	$\ell^* \to \ell\,\gamma$	1) acp pair $\ell^+\ell^-$ + 1 or 2 hard γ's 2) bump in $m^*_{\ell\gamma}$	$m_{\ell^*} \lesssim 2$ GeV [4] $\lambda^2 < 10^{-3}$	$m_{\ell^*} \lesssim 25$ GeV
	$e^+e^- \to \nu_\ell^* \overline{\nu_\ell^*}$	$250 \times \left(\frac{3\beta+\beta^3}{4}\right)$ [3]	If ν_ℓ^* massive, $\nu_\ell^* \to \ell^-(\ell^+\nu_\ell)$ $\to \ell + h$'s $\Gamma(h\text{'s})/\Gamma(\ell) \sim R$	1) acp $\ell\ell$ pairs 2) $\ell + h$'s 3) > 2 charged ℓ's 4) missing $p_\perp$ and E	$m < 1.2\text{-}2.2$ GeV	$m \lesssim 14$ GeV
(B) Sequential Leptons $\begin{pmatrix}\ell\\\nu_\ell\end{pmatrix},$ $\begin{pmatrix}\ell'\\\nu'_\ell\end{pmatrix},\ldots$	$e^+e^- \to \ell'^+\ell'^-$	$10^4 \times \left(\frac{3\beta-\beta^3}{2}\right)$	$\ell'^- \to \nu'_\ell(\ell\nu_\ell)$ $\to \nu'_\ell + h$'s $\Gamma(h\text{'s})/\Gamma(\ell) \sim R$	1) acp $\ell\ell$ pair 2) $\ell + h$'s 3) missing $p_\perp$, E	$m_\ell < 1.2\text{-}2.2$ GeV [9]	$m_\ell \lesssim 14$ GeV

[1] General searches: M. L. Perl, SLAC-PUB-1062 (1972); Decays and Production: Y. S. Tsai, Phys. Rev. D4, 2821 (1971); K. J. Kim and Y. S. Tsai, Phys. Lett. 40B, 665 (1972).

[2] S. V. Golovkin et al., paper No. 848, XVI Intl. Conf. on HEP, Chicago (1972).

[3] A. M. Litke, Thesis, Harvard University, p. III-8 (1970).

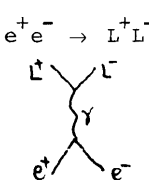[4] C. Bacci et al., Phys. Lett. 44B, 530 (1973); Super-Adone Proposal; DESY Seminar.

Particle	Production Mechanism	Rate per $\left\{\begin{array}{l}10^{38}\ cm^2 \\ 10^4\ \mu^+\mu^-\end{array}\right.$	Decay Modes/ Branching Ratios	Experimental Signatures	Present Limits	PEP Limits
HEAVY __LEPTONS__ (contd.)						
(C) Gauge Theory Leptons [5]	$e^+e^- \to L^+L^-$	$10^4 \times \left(\frac{3\beta-\beta^3}{2}\right)$	$L^+ \to \nu_\ell(\ell\nu_\ell)$ $\to L^o(\ell\nu_\ell)$ $(M_{L^+} > M_{L^o})$	Same as Sequential Leptons-- see (B)	$m_{M^+} \gtrsim$ 7-8 GeV[7] $m_{M^+} \lesssim 8$ GeV [9]	$m_{E^+} <$ 14 GeV
$\left(\begin{array}{c}\nu_e \\ e^- \\ E^o \\ E^+\end{array}\right)$	$e^+e^- \to L^o\overline{L^o}$	> 450 [6]	$\to \nu_\ell + h's$ $\to L^o + h's$		$m_{E^o} \gtrsim$ 1.2-2.2 GeV [9] $m_{M^o} < 4$ GeV	$m_{E^o} \lesssim 20$ GeV
$\left(\begin{array}{c}\nu_\mu \\ \mu^- \\ M^o \\ M^+\end{array}\right)$	$e^+e^- \to L^o\overline{\nu_\ell}$	> 200 [6]	$L^o \to \ell^-(\ell\nu_\ell)$ $\to \ell^- + h's$ $\to \nu_\ell + h's$ $\Gamma(h's)/\Gamma(\ell) \sim R$			
L = E or M						
(D) Quasi-stable leptons	$e^+e^- \to L^+L^-$	$10^{-4} \times \left(\frac{3\beta-\beta^3}{2}\right)$	Decay not seen in typical size detector $\tau \gtrsim 10^{-8} sec$	massive ($p_L < p_{BEAM}$), weakly interacting, collinear pairs	$m_L <$ 1 - 5 GeV [2]	$m_L \lesssim 15$ GeV

[5] Bjorken and Llewellyn Smith, Phys. Rev. __D7__, 887 (1973); Georgi and Glashow, Phys. Rev. Lett. __28__, 1494

[6] For Georgi-Glashow model with $\sin\theta_G = 1$ and M_{L^o} as indicated above; see Ahmed Ali, Stevens Institute of Technology preprint, 1974.

[7] B. C. Barish et al.

[8] Based on $(g-2)\mu$ experiments; see Primack and Quinn, Phys. Rev. __D6__, 3171 (1972).

[9] Washington Meeting APS SPEAR Report (April 1974); Drito et al., Phys. Lett. __48B__, 165 (1974); Bernardini et al., Bonn Conference (August 1973).

Particle	Production Mechanism	Rate per $\begin{cases}10^{38}\ cm^2 \\ 10^4\ \mu^+\mu^-\end{cases}$	Decay Modes/ Branching Ratios	Experimental Signatures	Present Limits	PEP Limits
(2) CHARGED VECTOR BOSONS	(a) $e^+e^- \to$ w^+w^-	1000 for M_W = 13.8 GeV, assuming (i) charge form factor = 1, (ii) no magnetic moment, (iii) no quadrupole moment	$w^\pm \to \ell^\pm \nu$ $e^\pm \nu / \mu^\pm \nu \approx 1$ $w^\pm \to$ hadrons $w^\pm \to \varphi\gamma$ if $M_W > M_\varphi$ [φ = Higgs-scalar meson] $\Gamma(h's)/\Gamma(\ell) \approx R$	(a) Final states $\ell^+\ell^-\bar{\nu}\bar{\nu}$ $\ell^\pm\nu$ + h's Look for $\alpha c\bar{p}$ μe, ee, and $\mu\mu$ pairs in ratio 2:1:1; missing $p_\perp$ and E	Present: $M_W \gtrsim 13$ GeV νN-NAL [2] $M_W > 18\text{-}24$ GeV $pp \to \mu^\pm X$ ISR [3]	< 14 GeV
	(b) $e^+e^- \to$ $e^\pm\nu w^\mp$	[4,5] 5 for M_W = 13.8 GeV, 50 for M_W = 6 GeV		(b) $e^+e^-\nu\bar{\nu}$, $e^\pm\mu^\mp\nu\bar{\nu}$, $e^\pm\nu$ + h's with $\alpha c\bar{p}$ ee, $e\mu$ pairs; missing $p_\perp$ and E		< 30 GeV

[1] See for example N. Cabibbo and R. Gatto, Phys. Rev. 124, 1577 (1961).

[2] B. Aubert et al. "Test of Scaling in High Energy Neutrino Interactions," 6th Int. Symp on Electron and Photon Interactions, Bonn Aug. 1973, 2nd Aix-en-Provence Int. Conf. on El Particles, September 1973.
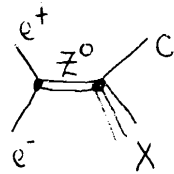
[3] G. Manning, Private Comminication.

[4] F. A. Berends and G. B. West, Phys. Rev. D1, 122 (1970), Phys. Rev. D2, 1354 (1970).

[5] Mikalian and J. Smith Phys. Rev. D4, 785 (1971).

[6] We have rewritten equation (19) of Berends and West (reference 4) to

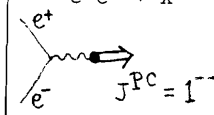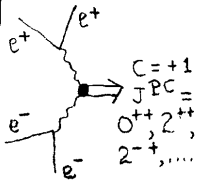demonstrate explicitly that, neglecting the electron mass terms, σ is only a function of M_W/E.
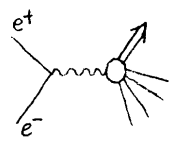
Particle	Production Mechanism	Rate per $\left\{\begin{array}{l}10^{38}\ cm^2\\10^4\ \mu^+\mu^-\end{array}\right.$	Decay Modes/ Branching Ratios	Experimental Signatures	Present Limits
(3) CHARM [1,2,3]	1) $e^+e^- \to C\bar{C}$	$\sim 1 - 100,$ $= \Lambda\bar{\Lambda}$	$C \to S + h's$ $(S = strange\ hadron)$ $\Gamma \sim \cos\theta_{Cabibbo}$ $C \to h's\ (non-$ $strange)$	1) Apparent viola- tion of strange- ness if $C \to h's\ (non-$ $strange)$ $\bar{C} \to h's +$ $strange\ hadron$	2 GeV < M < 10 GeV
	2) $e^+e^- \to C\bar{C}'X$ electromag- netic	~ 35 for $M_C =$ 10GeV ~ 1000 [4] above thresh- old $\approx$ inclu- sive baryon production	$\Gamma \sim \sin\theta_C$ $C \to S + (\ell\nu)$ $\Gamma(\ell\nu)/\Gamma(h's) \sim$ $10\% - 50\%$	$\Gamma \sim \sin\theta_C \cos\theta_C$ 2) Anomalous change in production of strange particles as E_0 passes through Charm threshold	
	3) $e^+e^- \to CX$ weak	~ 20 for $M_{Z^0} = 100$ GeV	$\tau \sim 10^{-12}$ sec	$\Gamma \sim \cos^2\theta_C$ 3) Signature 2) with an associated charged lepton	

[1] G. A. Snow, Nucl. Physics B55, 445-454 (1973).

[2] M. K. Gaillard, NAL Conf. 74/43-THY (April 1974).
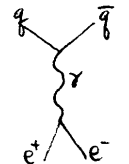
[3] S. L. Glashow, IV Intl. Conf. on Meson Spectroscopy.

[4] J. Marx, private communication.

Particle	Production Mechanism	Rate per $\begin{cases}10^{38}\,cm^2\\10^4\,\mu+\mu-\end{cases}$	Decay Modes/ Branching Ratios	Experimental Signatures	PEP Limits
(4) RESONANCES	(a) <u>Formation</u> $e^+e^- \to X$ $J^{PC} = 1^{--}$ E.g., high-mass vector meson daughters (v') of ρ,ω, and ϕ [1]	In principle, v' formation could account for a large fraction of $\sigma(e^+e^- \to$ hadrons) [1]	For vector mesons, $v' \to$ hadrons, ~100%; $v' \to \ell^+\ell^-, \lesssim$ few %.	Peaks in σ vs E_0 for particular final states.	30 GeV
	(b) <u>Two-photon exchange</u> $e^+e^- \to e^+e^-X$ $C = +1$ $J^{PC} = 0^{++}, 2^{++}, 2^{-+},\ldots$	5×10^5 with $2 < M_X < 6$ GeV [2,3]	Depends on specific resonance	For fixed E_0, peaks in M_X for specific states X, or, inclusively, for any X.	30 GeV
	(c) <u>Production</u> e^+ e^-	Depends on specific resonance	Depends on specific resonance	(v') Invariant mass peaks in multi-h, γ-h, ℓ-h, γ-ℓ, ℓ-ℓ, etc., combinations. E.g., see e* in $M(e\gamma)$ for $e^+e^- \to e^*e$ $(e^* \to e\gamma)$ (ii) Missing mass peaks.	30 GeV

[1] F. M. Renard, Montpelier (France) Univ. Report No. PM/74/3 (Feb. 1974)
[2] David W. G. S. Leith, SLAC-PUB-1440 (June 1974)
[3] J. Rosner, SLAC-PUB-1391 (1974)

Particle	Production Mechanism	Rate per $\left\{\begin{array}{l}10^{38}\ cm^2 \\ 10^4\ \mu^+\mu^-\end{array}\right.$	Decay Mode	Experimental Signatures	Present Limits	PEP Limit
(5) QUARKS[1]	$e^+e^- \to q\bar{q}$ $q \quad \bar{q}$ γ $e^+ \quad e^-$	$z^2\sigma_{\mu\mu}\left(\frac{3\beta-\beta^3}{2}\right)$ $\times$ FF	Low mass: may be quasi-stable High mass: may decay into hadron jets	(a) Anomalous dE/dx (for fractionally charged quarks) (b) Massive COL particle pair at low velocity (c) COL hadron jets	$\sigma < 10^{-35}\ cm^2$ for $M_q < 12$ GeV (for $p\bar{W} \to q\bar{q}X$ at $P_{inc} = 300$ GeV/c, $z = e/3$ or $2e/3$) [2] $\sigma < 3 \times 10^{-34}\ cm^2$, $z = e/3$, $M_q < 22$ GeV; $\sigma < 6 \times 10^{-34}\ cm^2$, $z = 2e/3$, $M_q < 13$ GeV (for $pp \to q\bar{q}X$ at $s \approx 2500$ GeV^2) [3] $\sigma < 10^{-39}\ cm^2$, $z = e/3$, $M_q < 4.7$ GeV; $\sigma < 2 \times 10^{-37}\ cm^2$, $z = 2e/3$, $M_q < 4.7$ GeV (for $p + A\ell \to q\bar{q}X$ at $P_{inc} = 70$ GeV/c) [4]	15 GeV

[1] For quark search review see L. W. Jones, Phys. Today 26, 30 (1973), No. 5.

[2] L. B. Leipuner et al., Phys. Rev. Letters 31, 1226 (1973).

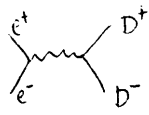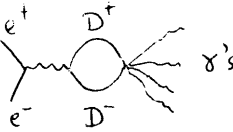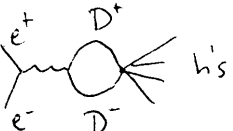[3] M. Bott-Bodenhausen et al., Phys. Letters 40B, 693 (1972).

[4] Yu. M. Antipov et al., Phys. Letters 30B, 576 (1969).

Particle	Production Mechanism	Rate per $\left\{\begin{array}{l}10^{38}\ cm^2\\ 10^4\ \mu^+\mu^-\end{array}\right.$	Decay Modes/ Branching Ratios	Experimental Signatures	Present Limits	PEP Limits
(6) GLUONS [1] (A) Neutral $J^{PC} = 1^{--}$ Color singlet SU_3 singlet (B) Vector [2] Color SU_3 Multiplet	Possibly if G is not a SU_3 singlet, or if symmetry breaking [3]	Not known [1], [2]	$G \to h's$ (like $\rho, \omega, \varphi \to h's$)	s dependent [4] structure in $\sigma_T(e^+e^- \to h's)$, $\sigma(e^+e^- \to \pi^+\pi^-)$, $\sigma(e^+e^- \to K\bar{K})$, etc.	none	30 GeV

[1] S. Weinberg, Phys. Rev. D8, 605, 4482 (1973). [2] Fritsch, Gell Mann, Leutwyler, Phys. Lett. 47B, 365 (1973).
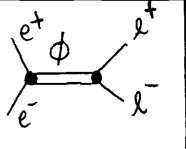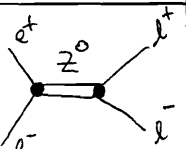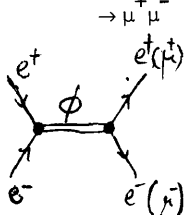[3] Chanowitz, Drell, Phys. Rev. Lett. 30, 807 (1973), Phys. Rev. D9, 2078 (1974).

[4] Dalitz, Talk given at PEP Summer Study, 1974.

Particle	Production Mechanism	Rate per $\left\{\begin{array}{l}10^{38}\ cm^2\\10^4\ \mu^+\mu^-\end{array}\right.$	Decay Modes/ Branching Ratios	Experimental Signatures	Present Limits	PEP Limits
(7) MONOPOLES [1,2] /DYONS	$e^+e^- \to D^+D^-$	No method to calculate rate because of the strong magnetic charge $(g^2/\hbar c \approx 137)$ [2], [4]	[4] (A) Free monopoles-- stable (rather unlikely) (B) Monopoles anni- hilate and γ's are emitted. Or, for Dyons, hadrons may be emitted.	(A) Magnetic charge-- accelerated in magnetic field. (B) Heavy ion- ization (C) Cerenkov radiation with elec- tric vector field direc- tion rotation of 90° from charged particles [8] (D) No reliable estimates on M, but large masses ($\sim$ 6 GeV to 137 × M_W) have been suggested [2,3] (E) Large number of γ's from D^+D^- annihilation [4]	$\sigma(pN \to p'N'D\bar{D})$ $< 1.4 \times 10^{-43} cm^2$ for $M_D < 5$ GeV [7]	$M_D < 15$ GeV

[1] Dirac, Phys. Rev. 74, 817 (1948).

[2] Schwinger, Science 165, 757 (1969).

[3] t'Hooft, CERN PREPRINT TH-1876 (1974).

[4] Newmeyer and Trefil, Phys. Rev. Lett. 26, 1509 (1971); Nuovo Cimento 89, 703 (1972); and Trefil, private communication.

[5] Alvarez, Eberhard, Ross and Watt, Science 167, 701 (1970).

[6] Fleischer, Price and Woods, Phys. Rev. 184, 1398 (1969).

[7] Adair, Proceedings of the 16th International Conference on High Energy Physics, Batavia, 4, 307 (1972).

[8] Shcherbakov, Proceedings of the 16th International Conference on High Energy Physics, Batavia, 2, 340 (1972).

Particle	Production Mechanism	Rate per $\left\{\begin{array}{l}10^{38}\ cm^2\\10^4\ \mu^+\mu^-\end{array}\right.$	Decay Modes/ Branching Ratios	Experimental Signatures	Present Limits	PEP Limits
(8) HIGGS SCALAR PARTICLE [2]	$e^+ \phi\ \ell^+$ / $e^-\ \ell^-$	$\sim 10^2$	$\varphi \to \ell^+\ell^-$ $\to$ h's	Sharp peak in[3] $\sigma_{\ell\ell}$ vs s ($\Gamma_\varphi \sim M_\varphi^3 \sim 1$ MeV for $M_\varphi = 1$ GeV)	$M > 0.5$ GeV (from K_L^0 decay) [4]	30 GeV
(9) NEUTRAL INTERMEDIATE BOSON [1]	$e^+ Z^0\ \ell^+$ / $e^-\ \ell^-$	$\sim 10^2$	$Z^0 \to \ell^+\ell^-$ $\to$ h's	1) Peak in $\sigma_{\ell\ell}$[3] vs s. 2) Interference between weak and EM production of $\mu\mu$, ee.		30 GeV
(10) LEE-WICK PARTICLE [5] (Heavy Photon)	$e^+e^- \to \varphi \to e^+e^-$ $\to \mu^+\mu^-$ (diagram)	$\frac{\Delta\sigma}{\sigma} = \pm \frac{8E^2}{\Lambda_\pm^2}$ in $e^+e^- \to \mu^+\mu^-$. (+) for Lee-Wick (−) for Heavy Photon	$\varphi \to e^+e^-$ $\to \mu^+\mu^-$ $\to$ hadrons (?)	1) Deviation from QED cross section and angular distribution in $e^+e^- \to e^+e^-$ 2) Deviation from QED total cross section in $e^+e^- \to \mu^+\mu^-$	25 GeV	200 GeV Virtual exchanges produce effects in QED reactions well below the threshold for production

[1] Weinberg, Phys. Rev. 19, 1265 (1967), Salam, Elementary Particle Physics, ed. Svartholm (Stockholm 1968), p. 367.

[2] Higgs, Phys. Rev. Letters 13, 508 (1964).

[3] J. Kirkby, talk given at PEP Summer Study (1974).

[4] From K_L^0 decay, see [3].

[5] Lee and Wick, Nucl. Physics B9, 209 (1969); A. Litke, Ph.D. Thesis, Harvard University (1970).

Particle	Production Mechanism	Rate per $\left\{\begin{array}{l}10^{38}\ cm^2 \\ 10^4\ \mu^+\mu^-\end{array}\right.$	Decay Modes/ Branching Ratios	Experimental Signatures	Present Limits
(11) TACHYON [1]	$e^+e^- \rightarrow T^+T^-$ $\rightarrow T^0\bar{T}^0$	?	?	(a) $T^{\pm}$ emit Cerenkov light at $\approx 90^{\circ}$ in electric field (b) $v > c$ (c) $M_T^2 < 0$ (d) COL particle pair	Photoproduction $(E_\gamma = 1.2\ MeV)$ $\sigma \lesssim 1.7 \times 10^{-33}\ cm^2$ for 0.5 e < tachyon charge < 1.9 e [2]

[1] O. M. P. Bilomink et al., Am. J. Phys. 30, 718 (1962); G. Feinberg, Phys. Rev. 159, 1089 (1967).

[2] T. Alväger and M. N. Kreisler, Phys. Rev. 171, 1357 (1968); M. B. Davis, M. N. Kreisler, T. Alväger, Phys. Rev. 183, 1132 (1969).

APPENDIX A

AN ALTERNATE SOURCE OF HIGH MASS TIMELIKE PHOTONS AND IMPLICATIONS

FOR NEW PARTICLE SEARCHES AT PEP

In this appendix we note that experiments soon to be carried out at the
FNAL will have important implications for the planning of new particle searches
at PEP. The experiments in question involve the reaction

$$p \; p \rightarrow \mu^+ \; \mu^- + X \qquad\qquad (A)$$

which we can represent pictorially as
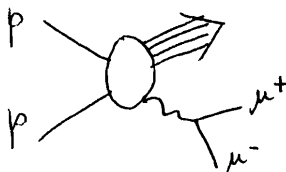
Measurement of the muon pair is actually a measurement of the flux of timelike
photons produced in hadronic reactions. If this timelike photon is indeed
the same as   produced at PEP, negative results for new particle searches
at FNAL will put stringent limits on the production of new particles F via a
reaction like

$$p p \rightarrow F^+ F^- + X \qquad\qquad \textbf{(B)}$$

The connection between the above two diagrams was first introduced by
Sculli and White[1] in considering quark searches. For the creation of a
pair of particles of charge Q, form factors F_1 and F_2 and anomalous magnetic
moment K, the ratio of the production cross section for the new particle to
the production cross section for muon pairs is

$$\frac{\left(d\sigma/dq^2\right)_{F\bar{F}}}{\left(d\sigma/dq^2\right)_{\mu\bar{\mu}}} = \left(\frac{Q}{e}\right)^2 \sqrt{1 - \frac{4M^2}{q^2}} \left\{ \left(F_1 + kF_2\right)^2 + \frac{2M^2}{q^2}\left(F_1 + \frac{kF_2 q^2}{2M^2}\right) \right\} \qquad \textbf{(1)}$$

where q^2 is the mass of the timelike photon and M the mass of the new particle. For a point particle with no anomalous magnetic moment, this reduces to

$$\left(\frac{Q}{e}\right)^2 \sqrt{1 - \frac{4M^2}{q^2}}\left(1 + \frac{2M^2}{q^2}\right) \tag{2}$$

so that the total cross section for production of the new particle in p-p collisions is

$$\sigma_{F\bar{F}} = \left(\frac{Q}{e}\right)^2 \int dq^2 \left(\frac{d\sigma}{dq^2}\right)_{\mu\bar{\mu}} \sqrt{1 - \frac{4M^2}{q^2}}\left(1 + \frac{2M^2}{q^2}\right) \tag{3}$$

The quantity $\left(\dfrac{d\sigma}{dq^2}\right)_{\mu\bar{\mu}}$ which appears in the integrand can be measured

in reaction (A), so that the expected cross section for production can be calculated. A negative search which places an experimental upper limit on $\sigma_{F\bar{F}}$ can be converted directly to a lower limit on the mass of the new particle.

Once this mass limit is calculated we can obtain a direct upper limit on the cross section which can be expected at PEP. Consider the reaction

$$e^+ e^- \to F^+ F^- \tag{C}$$

via
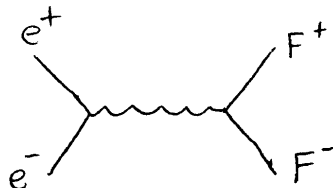
The cross section to produce a pointlike Dirac particle by process C is

$$\sigma(\text{process c}) = \frac{4\,\alpha^2}{3\,s}\,\beta\left(1 + \frac{M^2}{2s}\right). \tag{4}$$

In summary, a knowledge of the virtual photon flux in hadronic collisions can affect the planning of experiments at PEP. We wish to work through a concrete example here, although this involves some guesses at the form of $\left(d\sigma/dq^2\right)_{\mu\bar{\mu}}$. The ultimate use of the ideas presented here will depend on measurements of process (A) at FNAL.

The flux of muon pairs at BNL energies has been measured[2] . The general result can be summarized roughly by the equation

$$\frac{d\sigma}{dq} \sim \frac{C}{(q/GeV)^5} \qquad (5)$$

where the constant   C is approximately

$$C \approx 2 \times 10^{-32} \ cm^2/(GeV/c)$$

For the sake of argument, we assume that the function will continue to have this form to the highest energies. This assumption is probably incorrect, but the results we obtain will serve to illustrate the point we wish to make. Inserting Eq. (5) into Eq. (3), we obtain

$$\sigma_{F\bar{F}} = \left(\frac{Q}{e}\right)^2 \frac{C}{32 M^4} \int_1^\tau x\left(1 + \frac{x}{2}\right)\sqrt{1-x}\ dx \qquad (6)$$

where

$$x = \frac{4M^2}{q^2}$$

and

$$\tau = 4M^2/s$$

and we have neglected m_p^2/s.

Consider the example of the production of a quark of charge Q = 2/3 and mass M. The extension to other types of quasi-stable particles will be obvious. Assume that the present experimental upper limit of quark production persists up to 500 GeV, so that

$$\sigma_{F\bar{F}}(\text{process A}) < 10^{-37} \ cm^2 \qquad (8)$$

We then find that

$$M > 4.3 \ GeV \qquad (9)$$

522

This, in turn, when inserted into Eq. (4) will give an upper limit on the quark production cross section at PEP to be

$$\sigma_{F\overline{F}} \text{ (process C)} \lesssim (.64) \ \sigma \ (e^{+} e^{-} \rightarrow \mu^{+} \mu^{-}) \qquad (10)$$

for $S = (20 \text{ GeV})^{2}$.

As this example shows, the utilization of experimental evidence from p-p collisions can be very helpful in estimating upper limits on production cross sections at PEP, and could yield valuable information about which new particle searches ought to be carried out there and what sensitivity will be required from the apparatus.

REFERENCES

1)   J. Sculli and T. O. White, Phys. Rev. Lett. 27, 619 (1971)

2)   J. H. Christenson, G. S. Hicks, L. M. Lederman, P. J. Limon, and B. G. Pope, Phys. Rev. Lett. 25, 1523 (1970)

3)   R. Adair, Rapporteur's talk at XV International Conference on High Energy Physics, Chicago-NAL, 1973

APPENDIX B

DESIGN OF SPLIT FIELD MAGNET

ASSUMPTIONS: (See Figure 6)

Radius of good field	0.75m
Saturation field for iron	20kg
Gap seperation	2m
Maximum thickness of iron return annulus	.03m
Dimension of iron fins for return path	1.2 x 0.05m

From these assumptions, we calculate that the return yolk iron will saturate at 7 kg. Running the magnet at 5kg, and assuming that there is no reluctance in the return yolk, we find we need 8×10^5 amp-turns, divided between two coils. If the coils are made of copper, they will take a current density of 1000 amps/cm^2 , including an allowance for 20% of the area to be used for cooling water. The remainder of the design concerns matching the magnet to available power, and realistic power supplies. An example would be a coil of 20cmx20cm cross section, with 400 turns of 1cmx1cm water cooled wire carrying 1000 amps. Then the power dissipated is $\approx$ 1.3MW.

Number of coils	4
Number of turns/coil	400
Coil cross section	20cmx20cm
Current in coil	1000 amps.
Magnetic field	5 KG
Power	1.3 MW
Total weight of copper	6 tons
Total weight of steel	20 tons